Building and Collapse of the Cadomian Orogen: A Plate-Scale Model Based on Structural Data From the SW Iberian Massif

Diana Moreno-Martín[1] , Rubén Díez Fernández[2] , Ricardo Arenas[1], Esther Rojo-Pérez[1] , Irene Novo-Fernández[1,3], and Sonia Sánchez Martínez[1]

[1]Departamento de Mineralogía y Petrología, Instituto de Geociencias (UCM, CSIC), Universidad Complutense, Madrid, Spain, [2]Departamento de Geología y Subsuelo, Centro Nacional Instituto Geológico y Minero de España, CSIC, Salamanca, Spain, [3]Departamento de Mineralogía y Petrología (UGR), Universidad de Granada, Granada, Spain

Abstract The Cadomian Orogeny produced a subduction-related orogen along the periphery of Gondwana and configured the pre-Variscan basement of the Iberian Massif. The architecture of the Cadomian Orogen requires detailed structural analysis for reconstruction because of severe tectonic reworking during the Paleozoic (Variscan cycle). Tectonometamorphic analysis and data compilation in SW Iberia (La Serena Massif, Spain) have allowed the identification of three Cadomian deformation phases and further constrained the global architecture and large-scale processes that contributed to the Ediacaran building and early Paleozoic dismantling of the Cadomian Orogen. The first phase (D_{C1}, prior to 573 Ma) favored tabular morphology in plutons that intruded during the building of a continental arc. The second phase (D_{C2}, 573–535 Ma) produced an upright folding and contributed to further crustal thickening. The third phase of deformation (D_{C3}, ranging between ∼535 and ∼480 Ma) resulted in an orogen-parallel dome with oblique extensional flow. D_{C1} represents the crustal growth and thickening stage. D_{C2} is synchronous with a period of crustal thickening that affected most of the Gondwanan periphery, from the most external sections (Cadomian fore-arc) to the inner ones (Cadomian back-arc). We explain D_{C2} as a consequence of flat subduction, which was followed by a period dominated by crustal extension (D_{C3}) upon roll-back of the lower plate. The Ediacaran construction of the Cadomian Orogen (D_{C1} and D_{C2}) requires ongoing subduction beneath Gondwana *s.l.*, whereas its dismantlement during the Early Paleozoic is compatible with oblique, sinistral convergence.

1. Introduction

Part of the crystalline basement of Central and Southern Europe consists of rocks that were formed, deformed, metamorphosed, and recycled in an active-margin system, which involved a continental arc, accretionary wedges, back-arcs and other components (even cratonic basements in some cases) (Chantraine et al., 2001; Díez Fernández et al., 2019, 2022; Hajná et al., 2010). This arc system was built along the periphery of Gondwana during the Ediacaran and Early Paleozoic, and its dynamics is usually referred to as Cadomian Orogeny (D'Lemos et al., 1990; Eguíluz et al., 2000; Fernández-Suárez et al., 1999; Linnemann et al., 2000, 2008; Quesada, 1990). In the Iberian Massif, many interpretations regarding the Cadomian Orogeny have come from the analysis of Ediacaran-Early Paleozoic deposition of sedimentary series and coeval magmatism (Albert et al., 2015; Díez Fernández et al., 2010; Fernández-Suárez et al., 2014; Fuenlabrada et al., 2016; Rojo-Pérez et al., 2019, 2021). However, structural data is key to reconstructing the architecture of the Cadomian Orogen, its evolution, and to discussing the evolving plate kinematic model that may explain it. In SW Iberian Massif, studies that have contributed to distinguishing and characterizing Cadomian structures at the plate scale (e.g., suture zones) are gaining momentum (Arenas et al., 2018, 2021, 2022; Díez Fernández et al., 2019, 2022).

In Europe, obtaining structural data to discuss kinematic models of tectonic plates for the Ediacaran and Early Paleozoic Gondwana has some limitations. First, Cadomian records are geographically fragmented. Most of the rocks potentially bearing some structural imprint of that age are covered by Paleozoic, Mesozoic and Cenozoic strata, or even melted/intruded by later magmas (Eguíluz et al., 2000). This way, we observe pieces of a continental paleomargin and intra arc basin in North Armorican Massif in France (Chantraine et al., 2001), an accretionary wedge and tectonic mélange in Teplá-Barrandian Unit (Hajná et al., 2010, 2013, 2014; Sláma et al., 2008), a section of a forearc basin in Iberian Massif (Arenas et al., 2018), or pieces of a back arc marginal basin in Iberian Massif (Díez Fernández et al., 2022). Second, basement rocks have been involved in two additional orogenies other than the Cadomian, namely the Variscan (e.g., Ábalos & Eguíluz, 1992; Arenas et al., 2016;

Methodology: Diana Moreno-Martín, Rubén Díez Fernández, Ricardo Arenas, Esther Rojo-Pérez, Irene Novo-Fernández, Sonia Sánchez Martínez
Project Administration: Rubén Díez Fernández, Ricardo Arenas
Resources: Diana Moreno-Martín, Rubén Díez Fernández, Ricardo Arenas
Supervision: Rubén Díez Fernández, Ricardo Arenas
Validation: Diana Moreno-Martín, Rubén Díez Fernández, Esther Rojo-Pérez, Irene Novo-Fernández, Sonia Sánchez Martínez
Visualization: Diana Moreno-Martín, Rubén Díez Fernández
Writing – original draft: Diana Moreno-Martín
Writing – review & editing: Diana Moreno-Martín, Rubén Díez Fernández, Ricardo Arenas, Esther Rojo-Pérez, Irene Novo-Fernández, Sonia Sánchez Martínez

Azor et al., 2019; Bandrés et al., 2002; Díez Fernández et al., 2016; Expósito et al., 2003; Franke et al., 2017; Martínez Catalán et al., 2009, 2021; Matte, 1991; Quesada, 1990) and Alpine (e.g., de Vicente & Vegas, 2009; de Vicente et al., 2018). Third, the magmatic and metamorphic data regarding the Cadomian record suggest that this orogeny may span between ~750 and 500 Ma (Albert et al., 2015; Fuenlabrada et al., 2010; Linnemann et al., 2008, 2014; Pereira et al., 2006; Rodríguez-Alonso et al., 2004; von Raumer and Stampfli, 2008); therefore, several phases of deformation and evolving plate scenarios are expected. The fragmentary record of the Cadomian Orogen is pending to be discussed considering solid structural grounds that acknowledge both the potential complexity of Cadomian tectonics alone and the restoration of deformation that followed. Recognition of individual Cadomian phases of deformation as well as their dating along Europe is not always homogeneous. The use of different dating techniques should not preclude correlation if the data are accurate, as the choice of technique should not be the sole determinant of accurate results and robust correlation. However, the use of different techniques with their associated corresponding margin of error can slightly distort the data and make it difficult to correlate different metamorphic events. However, despite all of this, it is possible to make an approximation to perform a comparative analysis of the tectonic processes as well as their ages. The different pulses of crustal thickening and thinning observed in the Iberian Massif seem to be diachronous relative to those observed in other parts of Europe (Figure 1a). However, in order to build a tectonic model for the Cadomian evolution of Europe, we need to identify the major tectonic processes in each section of the Cadomian Orogen.

The SW part of the Iberian Massif (Figure 1a) occupied a peripheral position across the margin of Gondwana during the Cadomian Orogeny (Bandrés et al., 2004; Dörr et al., 2002; Drost et al., 2004; Henriques et al., 2015; Rubio-Ordóñez et al., 2015). This part is poorly affected by Alpine deformation (de Vicente et al., 2018; Jolivet et al., 2008). Accordingly, it represents an excellent candidate for tracking plate interactions between Gondwana and a subducting plate back in the Ediacaran and Early Paleozoic times. SW Iberia contains several exposures of Ediacaran rocks flanked by Paleozoic rocks, so it is possible to track the post-Cadomian deformation that affected the region and restore it to observe the primary geometry of Cadomian structures. This study includes a structural analysis of Cadomian-related rocks exposed in SW Iberia to distinguish between their Cadomian deformation and later imprints. The Cadomian record was integrated into a kinematic model of tectonic plates that discusses the processes that contributed to orogenic building and those that led to its dismantlement. The large-scale processes proposed in this work are tested against the main stages of Cadomian tectonic activity documented in other parts of Europe.

2. Geological Setting

The Iberian Massif is the southernmost part of the Variscan Orogen (Figure 1a), which resulted from the collision between Gondwana, Laurussia, and other peripheral terranes during the Devonian and Carboniferous (Arenas et al., 2016; Díez Fernández et al., 2016; Martínez Catalán et al., 2009; Matte, 2001; Ribeiro et al., 2007). The Iberian Massif is mostly made of crust that belonged to the Gondwana paleocontinent (D'Lemos, et al., 1990 Murphy et al., 2006; Stampfli et al., 2013). Such crust was fragmented into peripheral terranes during the Neoproterozoic and lower Paleozoic (Nance et al., 1991, 2010) to be transferred back again to their parental continent as a collection of far-traveled tectonic nappes during the Variscan Orogeny (Arenas et al., 2014, 2016; Díez Fernández et al., 2015, 2016; Martínez Catalán et al., 2009; Matte, 1991). The early history of these peripheral terranes, including their initial fragmentation, is related to subduction of oceanic crust beneath Gondwana and the dynamics of a continental arc system during Neoproterozoic-Cambrian times (Albert et al., 2015; Arenas et al., 2018, 2022; Bandrés et al., 2004; Díez Fernández et al., 2010, 2019, 2022; Dörr et al., 2002; Eguíluz et al., 2000; Henriques et al., 2015; Linnemann et al., 2008; Pereira et al., 2006, 2023; Quesada, 2006; Rojo-Pérez et al., 2019, 2022; Rubio-Ordóñez et al., 2015). This orogenic cycle (Cadomian Orogeny) led to a period of extension and related magmatism throughout the Iberian margin of Gondwana (Expósito et al., 2003; Linnemann et al., 2000; Rojo-Pérez et al., 2022), which culminated with the opening of the Rheic Ocean (Nance et al., 2010). The Cadomian processes proposed in the Iberian Massif left a record in the fragments of the Cadomian Orogeny found throughout the European Variscan belt. Cadomian structures and metamorphism suggest accretion and subsequent extension in the Armorican Massif (Chantraine et al., 2001), the Bohemian Massif (Hajná et al., 2010, 2013, 2014; Linnemann et al., 2008, 2014; Sláma et al., 2008) and Iberian Massif (Díez Fernández et al., 2019, 2022).

The SW Iberian Massif contains evidence of Cadomian deformation, metamorphism, and magmatism. In the Ediacaran series of SW Iberia, isotopic systems and minerals have yielded Neoproterozoic ages (600–550 Ma,
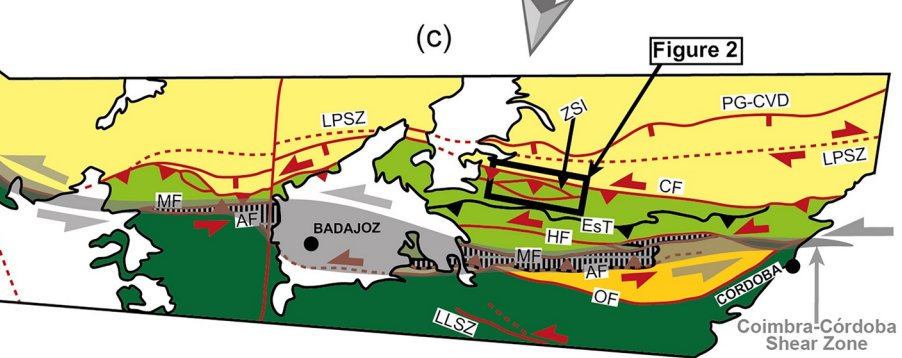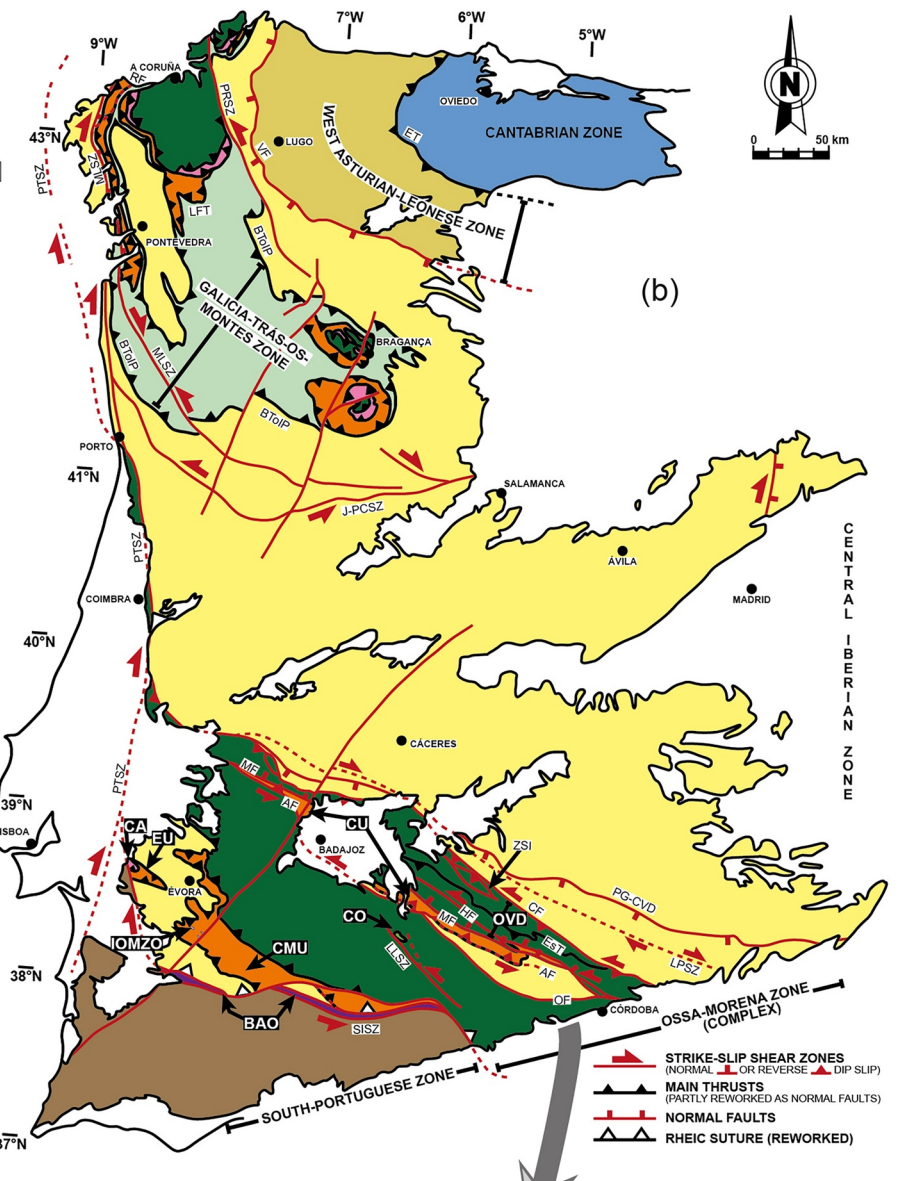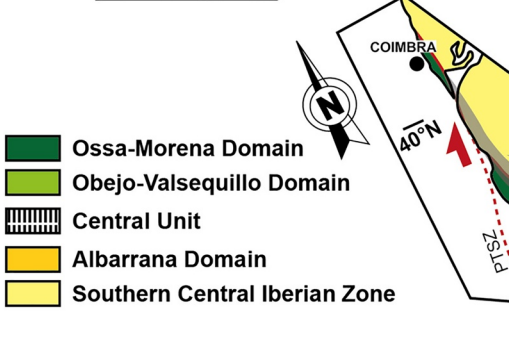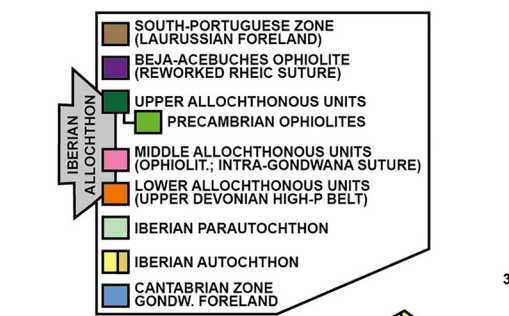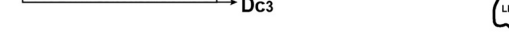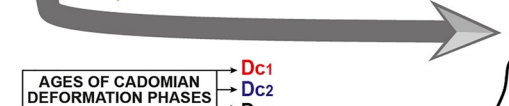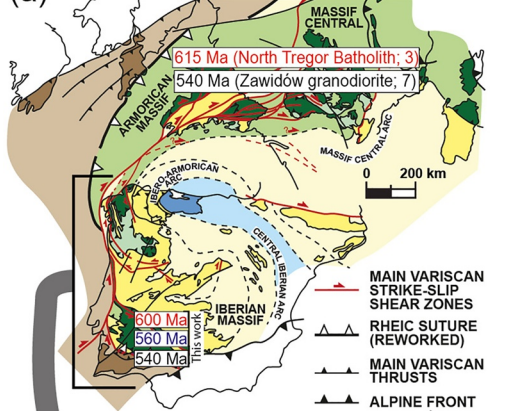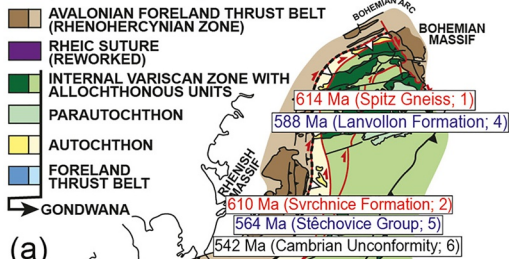
Figure 1.

Arenas et al., 2018, 2022; Blatrix & Burg, 1981; Dallmeyer & Quesada, 1992). The recognition of regional unconformities along the base of the latest Ediacaran through to the Ordovician has provided evidence of Cadomian deformation events, implying crustal thickening and/or thinning (Díez Fernández et al., 2019, 2022; Pereira

et al., 2006, 2023). In SW Iberia, Cadomian magmatism includes moderately basic to acidic igneous rocks, and bears the geochemical imprint of a supra-subduction zone setting (Rojo-Pérez et al., 2022, 2024).

The Obejo-Valsequillo Domain represents the northern section of a thrust stack formed during the Variscan Orogeny (Díez Fernández & Arenas, 2015; Díez Fernández et al., 2021; Figure 1b). A late Variscan fault system juxtaposes this domain against the Central Iberian Zone (Figure 1c; Apalategui & Pérez-Lorente, 1983; Díez Fernández & Arenas, 2015; Martín Parra et al., 2006), which is widely considered to be an inner section of the margin of Gondwana with respect to the rest of the SW Iberian Massif during the Variscan Orogeny (Díez Fernández et al., 2016; Pereira et al., 2012; Ribeiro et al., 2007; Simancas et al., 2009). The Obejo-Valsequillo Domain is featured by Ediacaran to lower Paleozoic rocks that bear imprints of Cadomian tectonics (e.g., Ábalos & Eguíluz, 1992; Apalategui & Pérez-Lorente, 1983; Arenas et al., 2022; Bandrés et al., 2004; Díez Fernández et al., 2019, 2022; Eguíluz et al., 2000; Sánchez-Lorda et al., 2016), some of which are arguably linked to ophiolite accretion and obduction (Arenas et al., 2022; Díez Fernández et al., 2022). Within this domain, the La Serena Massif consists of an exposure of Ediacaran and Paleozoic rocks (Figure 1c). The geological record of this massif has been divided into Cadomian and Variscan histories (Bandrés, 2001; Bandrés et al., 2004; Eguíluz et al., 1999; Ordóñez Casado, 1998). The geochronology, petrology, and regional lithostratigraphy of the rocks within this massif have been addressed in several studies (see Section 2.1). However, a study of the structure and tectonometamorphic evolution of the La Serena Massif aimed to distinguish between its Cadomian and Variscan imprints is pending, which is the core of this work.

2.1. Lithostratigraphy of the Study Area

Previous descriptions and subdivisions of the local lithostratigraphy of the La Serena Massif have been considered to map the bedrock of the study area (Apalategui et al., 1988; Bandrés, 2001; Castro, 1988; Herranz Araújo, 1985; Insúa Márquez et al., 1991; Pieren, 2000; Sánchez-Cela & Gabaldón, 1977). We deviated a little from their grouping of units, mostly in what primarily intrusive igneous rocks is concerned, where we preferred a different gathering of rock types in order to make meaning structural patterns emerge. In the following sections, we present the main petrological and stratigraphic features of the units considered in this work in the map and cross-sections of Figure 2.

2.1.1. Phyllites and Quartzites of Serie Negra Group

The Serie Negra Gp. is composed of intercalations of meta-sandstones, schists and black-greyish phyllites, and quartzites (Figures S1a, S2a, and S2b in Supporting Information S1). This series is considered to have been deposited in a turbiditic system and a siliciclastic platform formed in an active margin setting (Bandrés, 2001; Eguíluz, 1988; Pieren, 2000). The Serie Negra Gp. represents the host to the igneous rocks (as described in Sections 2.1.2 and 2.1.3). Some of these igneous rocks have been dated to 573 ± 14 Ma (zircon U-Pb age, Ordóñez Casado, 1998); therefore, this part of the Serie Negra Gp. must be older.

2.1.2. Porphyritic Metagranites and Augen Felsic Gneisses

Porphyritic coarse- to very coarse-grained metagranites are composed of K-feldspar, quartz, plagioclase (albite to oligoclase), and biotite (Figure S2c in Supporting Information S1) (Bandrés, 2001; Castro, 1988; Ordóñez Casado, 1998). Their texture is mostly cataclastic (Figure S2c in Supporting Information S1) and occasionally mylonitic (Figures S2d and S2e in Supporting Information S1). The latter texture was observed in small domains (2–10 cm) formed by shear zones. In these domains, the granites are deformed into mylonitic rocks and have asymmetric structures, such as sigma-type porphyroclasts, S-C, and S-C′ structures (Figure S1b in Supporting Information S1). The granites exhibit mingling textures with basic igneous rocks (diorites, tonalites, and gabbros) (Figure S1c in Supporting Information S1). The granites were dated c. 573 ± 14 Ma (zircon U-Pb age, Ordóñez Casado, 1998).

Figure 1. (a) Map of the Variscan Orogen. It contains references to the age of the main Cadomian deformation events, including the name of the units/formations that recorded it. References in red, pale purple, and black refer to D_{C1}, D_{C2}, and D_{C3}, respectively. The numbers (1–7) indicate the reference from the following list: 1—Lindner and Finger (2018); 2—Sláma et al. (2008); 3—Graviou et al. (1988); 4—Egal et al. (1996); 5—Drost et al. (2004); 6—Sláma et al. (2008); 7—Bialek et al. (2014). (b) Geological map of the Iberian Massif (Díez Fernández & Arenas, 2015). (c) Location of the study area in a regional map of SW Iberian Massif (Díez Fernández et al., 2021). Abbreviations: AF—Azuaga Fault; BToIP—Basal Thrust of the Iberian Parautochthon; BAO—Beja–Acebuches Ophiolite; CA—Carvalhal Amphibolites; CF—Canaleja Fault; CMU—Cubito–Moura Unit; CO—Calzadilla Ophiolite; CU—Central Unit; EsT—Espiel Thrust; EU—Escoural Unit; ET—Espina Thrust; HF—Hornachos Fault; IOMZO—Internal Ossa-Morena Zone Ophiolites; J–PCSZ—Juzbado-Penalva do Castelo Shear Zone; LFT—Lalín-Forcarei Thrust; LPSZ—Los Pedroches Shear Zone; LLSZ—Llanos Shear Zone; MLSZ—Malpica–Lamego Shear Zone; MF—Matachel Fault; OF—Onza Fault; OVD—Obejo–Valsequillo Domain; PG–CVD—Puente Génave–Castelo de Vide Detachment; PRSZ—Palas de Rei Shear Zone; PTSZ—Porto–Tomar Shear Zone; RF—Rías Fault; SISZ—South Iberian Shear Zone; VF—Viveiro Fault; ZSI—Zalamea de la Serena Imbricates.
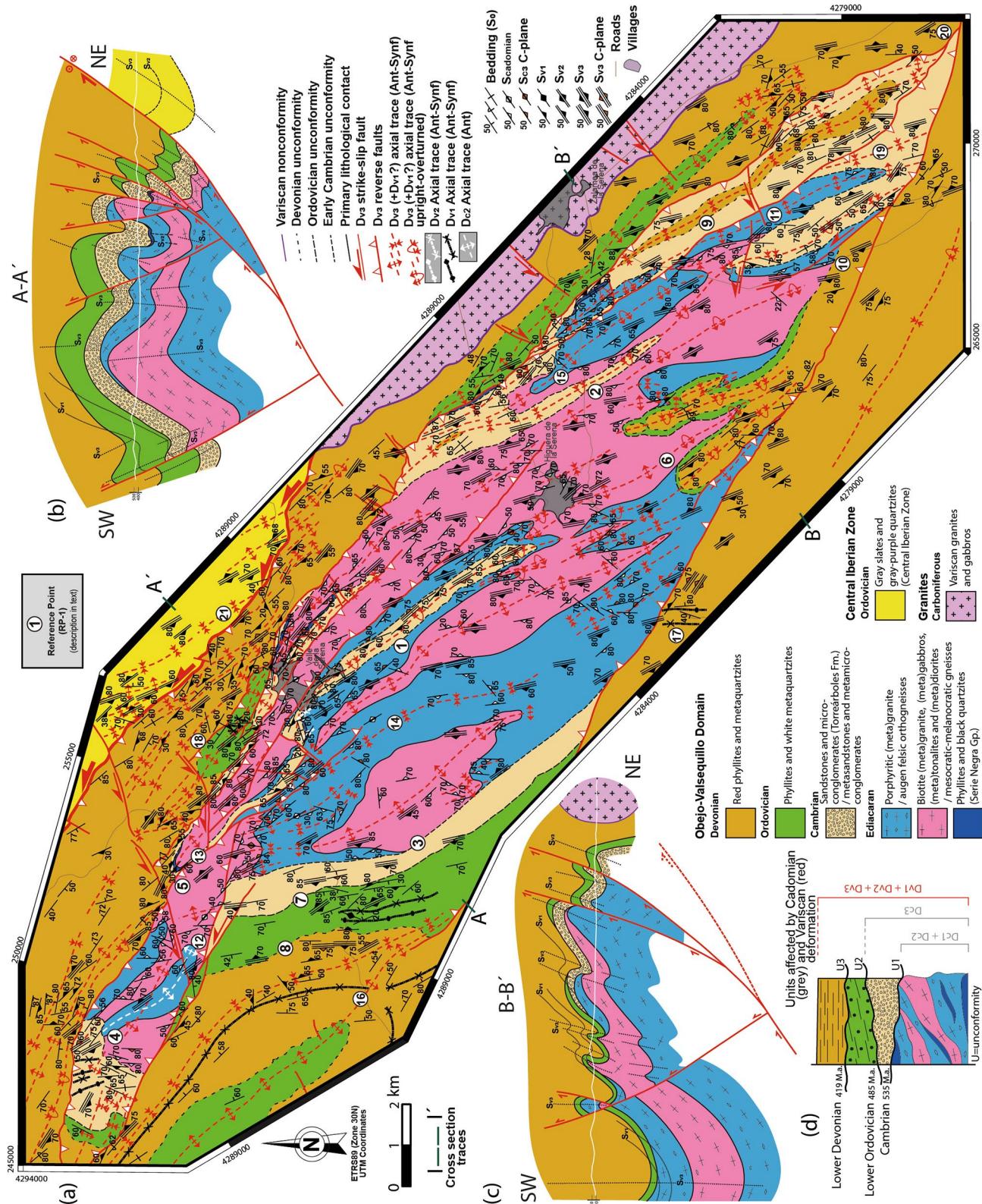
Figure 2. (a) Geological map with the planar structures in the study area. (b and c) Cross sections showing the main structures. (d) Lithostratigraphic column of the study area showing the ages of the unconformities and the lithologies affected by the structures generated during each phase of deformation.

2.1.3. Mesocratic-Melanocratic Gneisses

We grouped the remaining granitic lithologies (with intermediate-basic composition), and separated them from felsic granites. The igneous rocks of intermediate-basic composition are formed by biotite granites, tonalites, diorites, and gabbros. The biotite granites are fine-grained and are composed of biotite, quartz, feldspar, plagioclase, and opaque minerals. The diorites are formed by plagioclase, feldspar, and amphiboles (sometimes with pyroxene cores; Figure S2f in Supporting Information S1). The classification of diorites includes several types of adamellite and diorite (Castro, 1988). The most abundant is trondhjemite-type quartzdiorite, although there are also monzonites and more alkaline, undersaturated terms (Sánchez-Cela & Gabaldón, 1977). The tonalites are fine-grained and are composed of quartz, plagioclase, hornblende, and biotite, and are less abundant than the diorites (Castro, 1988; Sánchez-Cela & Gabaldón, 1977). Gabbros are composed of plagioclase, pyroxene, and occasionally very little quartz (leucocratic gabbros), and their texture is cataclastic (Figure S2g in Supporting Information S1) or occasionally mylonitic (Figure S2h in Supporting Information S1). In contact with the felsic granites, a mingling texture (Figure S1d in Supporting Information S1) and dikes of basic composition, such as diabase (Figure S2i in Supporting Information S1), were observed (Castro, 1988).

2.1.4. Torreárboles Formation (Early Cambrian)

This unit includes metaconglomerates and metasandstones (metaarkoses and quartz-rich metaarenites) (Figures S2j–S2l in Supporting Information S1). Metasandstones are composed of abundant quartz and K-feldspar (major microcline), ranging between 1 and 8 mm in size, filled on a partially recrystallized clay-micaceous matrix. It should be noted that plagioclase is present as an accessory (Sánchez-Cela & Gabaldón, 1977). Cross-bedding was observed in the weakly strained sections (Figure S1e in Supporting Information S1). The metaconglomerates are composed of sub-rounded to rounded clasts ranging between 2 and 8 cm, generally of quartz and quartzite, and to a lesser extent granitic porphyry, black quartzite, and slate (Sánchez-Cela & Gabaldón, 1977). According to its fossil content, the age of this formation is Early Cambrian (Liñán, 1984; Liñán & Palacios, 1983; Liñán et al., 1984).

2.1.5. Phyllites and Quartzites (Ordovician)

This succession consists of phyllites and white quartzites (Figure S1f in Supporting Information S1) (Apalategui et al., 1988). At its base, the succession includes an alternation of layers of quartzite and phyllite not thicker than a few centimeters. In the upper part, white quartzites occur as layers several meters thick alternating with minor phyllites. Cross-bedding was observed in the quartzite section (Figure S1f in Supporting Information S1). This succession shows very high lithostratigraphic affinity with the so-called Armorican Quartzite, so their sedimentary protoliths have been considered to have been deposited in a shallow marine siliciclastic platform during the Ordovician period. Contact metamorphism was observed close to the Late Carboniferous-Early Permian plutonic rocks that occur in the NE of the study area (Los Pedroches batholith; Figure S2m in Supporting Information S1).

2.1.6. Red Phyllites and Quartzites (Early Middle Devonian)

The lower part of this unit contains bioclastic marbles (not always present), followed by multi-colored phyllites and caramel-colored quartzites (Figures S1g–S1i in Supporting Information S1), whereas the upper part is composed of quartzites and ferruginous, red meta-sandstones, and minor phyllites (Figures S1j–S1l, S2n, and S2o in Supporting Information S1). The marbles contain brachiopod fauna fossils and, to a lesser extent, crinoids, bryozoans, and corals dated at Early Devonian (Apalategui et al., 1988). The upper part of this succession is analogous to a detrital succession from which Middle Devonian fossils were found (Apalategui et al., 1988).

2.1.7. Gray Phyllites and Quartzites of the Central Iberian Zone (Ordovician)

This series includes black, gray, and purple phyllites interbedded with levels of sandy slates, quartzites, and sandy bars alternating with caramel-colored quartzites (Figures S1m–S1q in Supporting Information S1), marble, and calc schist (Insúa Márquez et al., 1991). Quartzites appear in the lower layers alternating with silty slates. Marble presents bedding in layers of 1–2 m with interspersed metapelitic levels. This series has been considered Middle Ordovician-Silurian in age based on regional correlation (Insúa Márquez et al., 1991).

3. Tectonometamorphic Data

In the study area, Cadomian and Variscan deformation and metamorphism occurred, resulting in three major unconformities and six phases of deformation, that generated planar and linear structures (Figures 2 and 3).
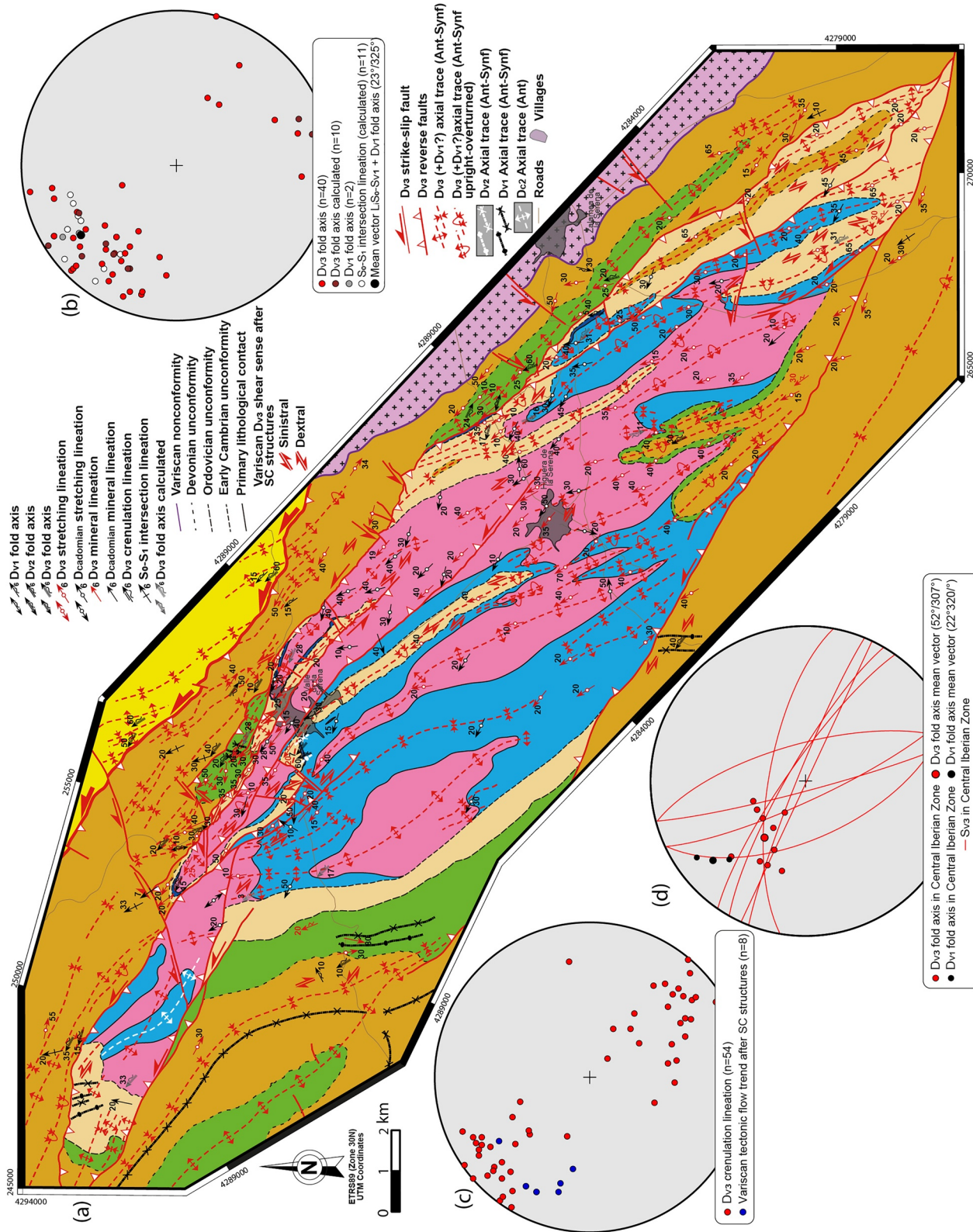
Figure 3. (a) Geological map with the linear structures in study area. (b–d) Stereograms with structural data. (b) D_{V3} fold axis measured and calculated from bedding, D_{V1} folds axis measured and S_0–S_1 intersection lineation representing the axes of D_{V1} folds. (c) D_{V3} crenulation lineation and Variscan tectonic flow calculated after S-C structures. (d) D_{V2} and D_{V3} fols axis in Central Iberian Zone.

3.1. Unconformities

The base of Torreárboles Fm. may contact either felsic (RP-1; Figure 2) or intermediate to melanocratic Cadomian igneous rocks (RP-2; Figure 2). This base cuts the boundaries between porphyritic and mesocratic metagranites (RP-3; Figure 2), sometimes at a high angle (RP-4; Figure 2), and cuts the contacts between the Serie Negra Gp. and the Cadomian igneous rocks (RP-5; Figure 2). Accordingly, the Torreárboles Fm. lies uncomformably over the Serie Negra Gp. and an ensemble of Cadomian metaigneous rocks.

The base of the Ordovician succession cuts the contacts between the Cadomian metaigneous rocks (RP-6; Figure 2) or rests directly onto the Torreárboles Fm. (RP-7; Figure 2).

The Devonian strata features another unconformity, since the base of the Devonian series generally lies on the Ordovician succession (RP-8; Figure 2), but it can also occur over the Torreárboles Fm. (RP-9; Figure 2), and Cadomian igneous rocks (RP-10; Figure 2).

3.2. Cadomian Structures

The structures described below do not affect lithologies younger than Torreárboles Fm. This criterion and the unconformity at the base of the Ordovician series were used to distinguish and integrate these structures as part of the Cadomian record sensu lato. Three Cadomian phases of deformation are observed in the study area (D_{C1}, D_{C2}, and D_{C3}).

3.2.1. D_{C1} (S_{C1})

Patches of metasedimentary rocks of the Serie Negra Gp. experienced contact (thermal) metamorphism, as typified by cordierite-bearing hornfels after foliated phyllites. In these cases, cordierite occurs as a post-kinematic, sub-idiomorphic, and poikiloblastic mineral that includes foliation defined by white mica, quartz, and minor biotite and opaques (Figure S2b in Supporting Information S1; S_{C1}). This thermal metamorphism is missing in the Cambrian sedimentary succession that lies unconformably on top, even in outcrops located a few tens of meters away from these hornfels. Accordingly, we link this contact metamorphism to the nearby Cadomian igneous rocks, with the previous foliation (S_{C1}) being the oldest evidence of deformation observed in the study area. The intrusion of igneous bodies and Sc_1, which occurred during D_{C1} and affected the Serie Negra Gp., predates the Torreárboles Fm., as none of them are observed within this formation.

3.2.2. D_{C2}

The existence of a second phase of Cadomian deformation is based on the unconformable nature of the Torreárboles Fm. The varying lithologies that occur under the basal contact of this Cambrian series suggest that some type of deformation is needed to expose the pre-Cambrian rocks before Cambrian sedimentation. Mapping of the Cadomian igneous rocks suggests that they represent roughly tabular-shaped bodies, as inferred from the sinuous pattern of their boundaries and sub-parallelism to foliation, both of which usually define the same folds as the overlying metasedimentary series (Figure 2). Such tabular structures were truncated by the base of the Torreárboles Fm. at several points (e.g., RP-3, 4, 11; Figure 2), indicating that some of the tabular shapes have been formed prior to the Cambrian strata. A critical observation can be made at RP-4 (Figure 2a), where the main foliation observed in the Cadomian igneous rocks is folded into an antiform that is unconformably covered by the base of the Torreárboles Fm., which cuts at a high angle the foliation-parallel contacts defined by the metaigneous rocks. Figure 4a shows up to five levels of near-tabular metaigneous rocks (from A to E) that can be inferred from the structural analysis.

We performed a qualitative analysis of the obliquity between the base of the Torreárboles Fm. and contacts between the pre-Cambrian rocks (Figure 4a). The analysis is based on map patterns, such as crosscutting relationships between contacts and wedging of units, so that we can identify structures at the map scale. This analysis yielded different primary dip-directions for the pre-Cambrian rock ensemble relative to a roughly horizontal Torreárboles Fm. (deformation affecting Cambrian rocks must be restored). For instance, in the SW part of the map (RP-3; Figure 2), the dip of the contact between the melanocratic (D in Figure 4a) and felsic gneisses (C in Figure 4a) is shallower than the dip of the Torreárboles Fm. (note the wedging of felsic gneisses under the Cambrian strata). Accordingly, if we rotate the Cambrian strata to a horizontal geometry and tracked such rotation in the pre-Cambrian rocks, the latter would be roughly dipping to the NE before Cambrian sedimentation.
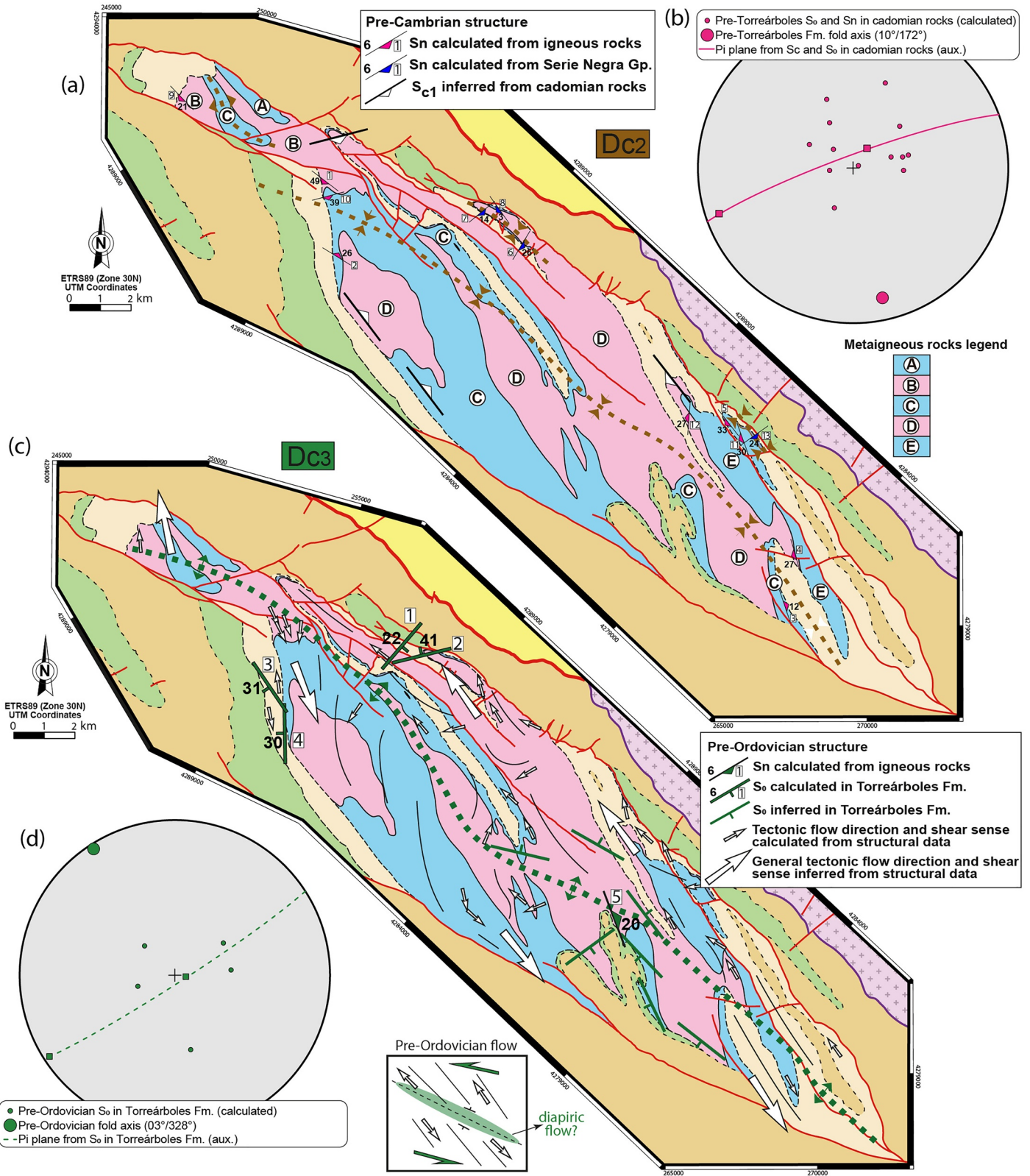
Figure 4.

In the N part (RP-4; Figure 2), the base of the Torreárboles Fm. rests on top and cuts the contact between felsic (C in Figure 4a) and melanocratic gneisses (B in Figure 4a). To the south, the contact defines an SE-plunging periclinal fold, and the Torreárboles Fm. is missing (RP-12; Figure 2), thus implying an S- to SSE-dipping direction of the pre-Cambrian rocks before Cambrian sedimentation. In the hinge zone of the NW-plunging antiform (RP-13; Figure 2), the SE wedging of the Serie Negra Gp. between the melanocratic gneisses and Torreárboles Fm. indicates an SE-dipping geometry for the pre-Cambrian rocks before Cambrian sedimentation.

The Torreárboles Fm. can be found along the rims and core of the pre-Cambrian rock set. The exposure of the Cambrian series at the core (RP-1; Figure 2) corresponds to the hinge zone of a synform, but that series is missing over the hinge zone of an equivalent synform that occurs to the W (RP-14; Figure 2). Given that the melanocratic gneisses around RP-14 (Figure 2) correspond to the same massif (D in Figure 4a), the occurrence of the Torreárboles Fm. to the E of RP-14 (at RP-1; Figure 2) can be explained by a SW-dipping geometry of the boundary between orthogneisses before Cambrian sedimentation. Torreárboles Fm. rests onto melanocratic gneisses (D in Figure 4a) at RP-2 (Figure 2), but those gneisses wedge toward the E between the base of the Cambrian series and the underlying felsic gneisses (E in Figure 4a). Such wedging occurs in the NE-dipping limb of an antiform (RP-15; Figure 2) and indicates an SW-dipping geometry for the contact between orthogneisses before Cambrian sedimentation. The collection of individual inferences for the geometry of the boundaries between orthogneisses before the Torreárboles Fm. was deposited supports a NW-SE trending synform (Figure 4a). This would not be the only fold attributable to this phase of deformation, since the antiform at RP-4 (Figure 2a) should be also part of the same fold family. We cannot rule out the existence of tectonic fabric associated with this folding (i.e., S_{C2}), but we did not find any foliation in the pre-Cambrian rocks that could be exclusively explained by such folding alone.

The quantitative restoration of bedding (Serie Negra Gp.) and foliations that rest unconformably under the Torreárboles Fm. suggests D_{C2} folds trending NNW-SSE (10°/172°; Figure 4a), which are analogous to the synform inferred from the qualitative analysis and the antiform at RP-4 (Figure 2a).

3.2.3. D_{C3} (S_{C3})

The identification of a third phase of Cadomian deformation is based on a collection of structures that are only observed in the Ediacaran metaigneous rocks, Serie Negra Gp., and Torreárboles Fm., plus the unconformable nature of the Ordovician succession.

The pre-Ordovician rocks show a foliation (S_{C3}) that is heterogeneously distributed throughout the study area. The penetrativeness and intensity of S_{C3} range between poorly developed foliation (Figures S1a and S1b in Supporting Information S1), even absence of shape-fabric (Figures S1c and S1d in Supporting Information S1), and mylonites (Figures S1r, S1s, and S2a in Supporting Information S1). S_{C3} in metaigneous rocks is a coarse foliation (shape fabric) that may be defined (depending on the protolith) by the preferred orientation of feldspar, plagioclase, quartz (ribbons), biotite, muscovite, amphibole, chlorite, and opaque minerals (e.g., Figures S2e and S2h in Supporting Information S1). S_{C3} is a schistosity in the metasedimentary rocks of the Serie Negra Gp., whereas in the metasandstones and metaconglomerates of the Torreárboles Fm. S_{C3} consists of a shape fabric ranging between rough and mylonitic foliation. In both cases, and depending on protolith, S_{C3} may be defined by the shape-preferred orientation of quartz (ribbons and segregates), biotite, muscovite, plagioclase, feldspar and opaque minerals (Figures S1i, S2a, and S2k in Supporting Information S1). The minerals that define S_{C3} can sometimes be observed as aggregates parallel to foliation, and their elongated shape, together with the long axis of individual metamorphic minerals and porphyroclasts (both in igneous and sedimentary rocks), define a stretching and mineral lineation (L_{C3}) mostly trending NW-SE (Figure 5a).

S_{C3} is associated with the development of asymmetric structures, including S-C-C′ structures (Figures S1r and S1s in Supporting Information S1), sigma objects (Figures S1a, S1b, S1r, S1s, S2e, S2h, and S2k in Supporting Information S1), and asymmetric folds with asymmetry reversal (Figure S1r in Supporting Information S1). The shear-sense inferred from these structures (Fossen & Cavalcante, 2017) and the stretching lineation was either

Figure 4. (a) Geological map highlighting the D_{C2} structure in the study area (brown dashed line corresponds to the axial trace of an upright synform). (b) Stereogram with pre-Torreárboles Fm. bedding and Cadomian foliation in Cadomian basement and fold axis calculated from the bedding and Cadomian foliation. (c) Geological map indicating the D_{C3} structure in the study area (green dashed line corresponds to the axial trace of an upright antiform) and tectonic flow direction calculated after Cadomian S-C structures. The numbers that accompany the calculated Sn and S_0 refer to those included in the database containing all the structural data (Moreno-Martín et al., 2023). (d) Stereogram with pre-Ordovician bedding in Torreárboles Fm. and fold axis calculated from the pre-Ordovician bedding in Torreárboles Fm.
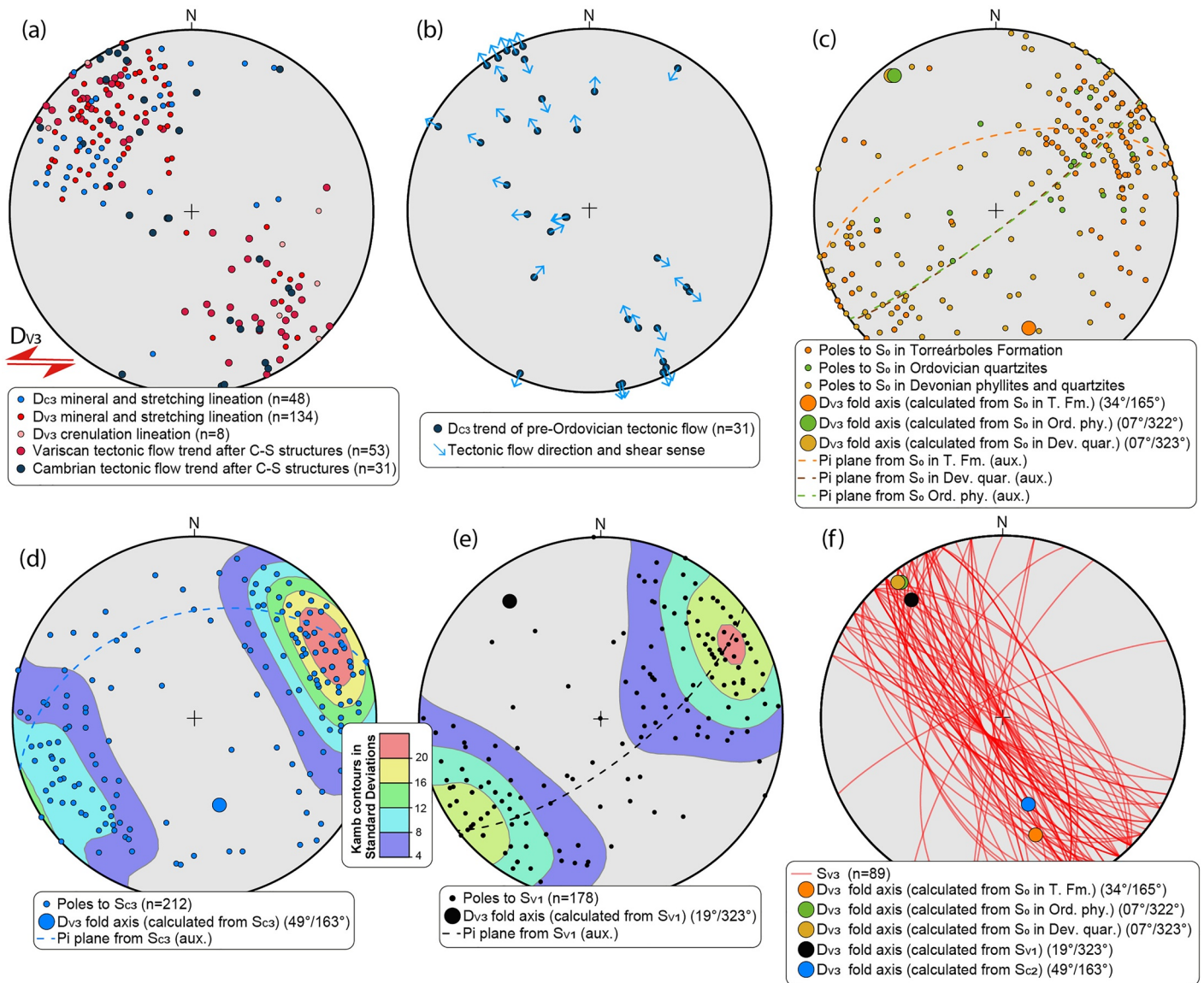
Figure 5. Stereograms with structural data from the study area. (a) D_{C3} mineral and stretching lineation. Note that the Cambrian tectonic flow inferred from these lineations fits the trend of D_{V3} mineral and stretching lineations and that of the tectonic flow vectors (LSC) calculated after C-S structures. (b) Lines and shear sense (calculated after C-S structures) defining the pre-Ordovician tectonic flow. (c) D_{V3} fold axes calculated from bedding in Torreárboles Fm., Ordovician quartzites, and Devonian phyllites and quartzites. (d) D_{V3} fold axis calculated from poles to S_{C3}. (e) D_{V3} fold axis calculated from poles to S_{V1}. (f) S_{V3} and D_{V3} fold axes calculated from bedding in Torreárboles Fm., Ordovician quartzites and Devonian phyllites and quartzites. Abbreviations: T. Fm.—Torreárboles Formation. Ord. phy.—Ordovician phyllites. Dev. quar.—Devonian quartzites.

top-to-the-NW or top-to-the-SE (Figure 5b). L_{C3} shows a trend parallel to Variscan linear structures (fold axes and lineations; Figure 5a), so it might have resulted from reorientation upon Variscan deformation. However, the trend of L_{C3} (Figure 5a) matches the trend of tectonic flow vectors (LSC) calculated for D_{C3} (Figure 5b).

We performed qualitative and quantitative restoration of the pre-Ordovician structure (Figure 4c). Qualitative restoration followed a procedure similar to that described in Section 3.2.2. The quantitative restoration was done by rotating Ordovician bedding to a horizontal geometry, using D_{V3} fold axis, while tracking such rotation in the planar structures of the lithologies below (either S_{C3} or bedding). The resulting pre-Ordovician structure consists of an antiform defined by bedding, lithological contacts between metaigneous rocks, and S_{C3}. The axial trace of this antiform is shown in Figure 4b, and its fold axis trends NW-SE (03°/328°; Figure 4d). The tectonic flow inferred from the asymmetric S_{C3} structures and the trend of L_{C3} is oblique to the hinge of this fold and is oriented

clockwise from its axial trace. The D_{C3} tectonic flow shows a bi-vergent pattern directed away from the hinge zone of the antiform (i.e., top-to-the-NW in the NE-dipping limb and top-to-the-SE in the SW-dipping limb).

3.3. Variscan Phases of Deformation and Their Interference

The set of structures presented below can be observed in pre-Paleozoic and Paleozoic metamorphic rocks.

3.3.1. D_{V1} Folds and Fabrics

D_{V1} generated folds that affected the Ediacaran through to the Devonian rocks. The D_{V1} folds are tight, overturned, and asymmetric (E-verging). Although many individual Variscan folds in the study area probably result from the addition of D_{V1} and homoaxial D_{V3} folds (see below), some D_{V1} folds can still be identified at the meso- to macroscale. When this is possible, D_{V1} folds tend to show N-S trending, as is the case for the type-1 interference pattern (Ramsay, 1967) at RP-16 and RP- 4 (Figure 2), or the folds at RP-17 and RP-18 (Figure 2) (bedding is folded but the dip-direction of the first Variscan foliation is not), among others. D_{V1} folds show axial planar foliation (S_{V1}) (Figures S1j and S2o in Supporting Information S1). In Ordovician and Devonian rocks, S_{V1} is schistosity defined by quartz, muscovite, opaque minerals, chlorite, plagioclase, and minor biotite.

3.3.2. D_{V2} Fabrics

D_{V1} structures and bedding are transposed by flat-lying crenulation cleavage (S_{V2}; Figures S1g and S2o in Supporting Information S1) and associated crenulation lineation. These fabrics are spatially related to NNW-SSE-trending folds, all of which are local and have no bearing on the structure at the macroscale. S_{V2} is defined by the mechanical reorientation of previous minerals (e.g., S_{V1}) and newly formed quartz, chlorite, white mica, and sericite.

3.3.3. D_{V3} Folds, Shear Zones and Fabrics

S_{C1}, S_{C3}, S_{V1}, and S_{V2} were affected by folds and faults. Faults can be high-angle, reverse, or purely strike-slip. These structures can be recognized in all rocks in the study area.

D_{V3} folds were observed at the macroscale (Figure 2), mesoscale (Figures S1j–S1l and S1t in Supporting Information S1), and microscale (Figures S2b, S2n, and S2o in Supporting Information S1). D_{V3} folds are upright to overturned, and their geometry ranges from tight to open (Figures S1j–S1l, and S1t in Supporting Information S1) (Figures 2b and 2n). Their axes trend NW-SE, while their plunge is dominantly to the NW and SE in the NW and SE parts of the study area, respectively (Figures 3a, 3b, 5c, 5d, and 5e). The D_{V3} fold axial planes are near-vertical, but the vergence changes accordingly, being to the NE (e.g., Figures 1u and S1v in Supporting Information S1) and SW (e.g., Figure S1l in Supporting Information S1) in the NE and SW sections, respectively. Despite this general tendency, the vergence changes locally in relation to the dip-slip tectonic transport of nearby D_{V3} shear zones. For instance, the vergence would be to the NE if the dip-slip component of a D_{V3} shear zone is directed to the NE.

The D_{V3} folds are accompanied by axial planar foliation (S_{V3}; Figures 2b and 2c), which occurs as subvertical crenulation cleavage (S_{V3}; Figures S2b, S2n, and S2o in Supporting Information S1). The strike of S_{V3} is NW-SE, and its dip-direction is NE or SW (Figures 2a and 5f). S_{V3} is defined by the reorientation and recrystallization of previous minerals, such as quartz, biotite, muscovite, plagioclase, and feldspar, plus newly formed quartz, muscovite, sericite, and opaque minerals. This foliation occurs alongside crenulation lineation formed at the expense of S_{C1}, S_{C3}, S_{V1}, and S_{V2} (Figure S1i in Supporting Information S1) and trending NW-SE (Figure 3c).

The D_{V3} shear zones strike NW-SE and are subvertical, usually dipping >60° to the NE or SW (Figures 2a–2c). These shear zones are accompanied by a set of shear zones that strike NE-SW to E-W, which usually connect several NW-SE trending shear zones along their trace. Most D_{V3} shear zones were first revealed by the presence of mylonites crosscutting along the boundaries of the Ediacaran and Paleozoic rocks, but they can also emerge from the mapping of lithological ensembles. Based on the mapping, we observed an upthrown movement of the upper block to most faults. Otherwise, a left-lateral component can be inferred. However, based on the direct observation of slickenlines plus kinematic indicators (sigma and delta objects, S-C structures; Figures S1b, S2d, S2j, and S2l in Supporting Information S1) and NW-SE-trending stretching lineation within mylonites (Figure 5a) (Figure S1h in Supporting Information S1), most shear zones can be classified as dip-slip faults, including a component of left-lateral and reverse movement. The D_{V3} mylonitic foliation is defined by recrystallized and newly formed quartz, muscovite, sericite, biotite, feldspar, and plagioclase.

The D_{V_3} reverse faults tend to be subparallel to D_{V_3} fold axial planes and S_{V_3}. However, the D_{V_3} fold axial planes can also be oblique and oriented clockwise from the D_{V_3} faults (e.g., RP-19; Figure 2). The D_{V_3} reverse faults tend to converge at the surface (RP-20; Figure 2), suggesting an overall imbricate structure for the fault system (Figures 2b and 2c; Figures S1u and S1v in Supporting Information S1). However, the tectonic transport of individual reverse faults indicates that the core of the study area corresponds to a major antiform exposed over a D_{V_3} pop-up structure (Figures 2b and 2c). Most major D_{V_3} antiforms (e.g., those with cartographic expression) tend to occur over hanging walls to D_{V_3} reverse faults, while D_{V_3} synforms usually occupy their footwalls.

3.4. Central Iberian Zone

The oldest rocks of the Central Iberian Zone included in this study are Ordovician (Insúa Márquez et al., 1991), so they are unable to provide direct constraints on the Cadomian evolution. Because these rocks are affected by Variscan deformation and metamorphism, they have been used to reinforce arguments to distinguish between Variscan and Cadomian deformation in the region.

The first phase of deformation corresponds to tight upright folds with an NNW-SSE fold axis trend (Figure 3d) and an associated axial planar foliation (Figure S1o in Supporting Information S1). This foliation is a schistosity defined by quartz, muscovite, chlorite, minor biotite, plagioclase, and opaque minerals. The second phase of deformation is characterized by a crenulation cleavage formed after the rotation of minerals from the previous foliation and newly formed quartz, muscovite, sericite, and opaque minerals. This fabric represents the main and dominant foliation in this section of the Central Iberian Zone. The third phase of deformation is typified by folds that affect all previous fabrics and occur alongside axial planar foliation. The axes of these folds trend NW-SE trend, and may show shallow to moderate plunge (52°/307°) (Figure 3d; Figure S1n in Supporting Information S1), likely due to the primary obliquity between the previous fabric and axial plane. This axial planar foliation is nearly vertical and is defined by quartz, muscovite, minor biotite, and opaque minerals. The sequence of Variscan phases of deformation and associated structures (and their associated fabrics) are referred D_{V_1} (S_{V_1}), D_{V_2} (S_{V_2}), and D_{V_3} (S_{V_3}).

S_{V_3} in the Central Iberian Zone is oriented clockwise from the boundary between the Central Iberian Zone and the Obejo-Valsequillo Domain, and so are the traces of D_{V_3} folds (RP-21; Figure 2). Such boundary cuts across the internal structure of both the Central Iberian Zone and the Obejo-Valsequillo Domain, including the D_{V_3} folds, so it corresponds to a late Variscan shear zone. This shear zone dips steeply to the SW (according to the mapping of its trace) and shows a similar relationship to S_{V_3} in both the Central Iberian Zone and the Obejo-Valsequillo Domain. This shear zone runs parallel to the rest of the D_{V_3} shear zones within the Obejo-Valsequillo Domain, even close to some of them (~1 km across the section, RP-21; Figure 2). Therefore, this boundary will also be tentatively considered as a sinistral shear zone with reverse dip-slip and imbricated with the rest of D_{V_3} shear zones of the Obejo-Valsequillo Domain (Figure 2b).

4. Discussion

The pre-Ordovician rocks constitute a pre-Variscan basement involved in the Variscan Orogeny, which is another contributor to the dismantling and dismembering of the Cadomian record. Variscan deformation modifies the Cadomian record on a regional scale; therefore, it is dealt with first to provide a frame for discussion.

4.1. Variscan Tectonics

Early Variscan deformation in the Devonian rocks of the Obejo-Valsequillo Domain is considered to be Late Devonian (Dallmeyer & Quesada, 1992; Garrote & Broutin, 1979; Sánchez-Cela & Gabaldón, 1977). This deformation is attributed to the shortening of an upper plate during continental subduction and collision (Díez Fernández et al., 2016). On the other hand, the D_{V_1} structures of the Central Iberian Zone would account for the progression of the same collision into the inner parts of the lower plate later in the Carboniferous (Rubio Pascual et al., 2013, 2016).

In the absence of absolute age data, the D_{V_2} structures in the Obejo-Valsequillo Domain and Central Iberian Zone can only be linked to the extension-related processes that affected the hinterland of the Variscan orogen between ~345 and 315 Ma (Arango et al., 2013; Díaz Azpiroz et al., 2004; Martínez Catalán et al., 2014; Moreno-Martín et al., 2022; Pereira et al., 2009, 2012; Rubio Pascual et al., 2013).

The set of D_{V3} structures in the study area is analogous to other strike-slip systems formed during the late stages of the Variscan Orogeny (∼315–305 Ma; Capdevila & Vialette, 1970; Díez Fernández & Martínez Catalán, 2012; Díez Fernández & Pereira, 2017; Expósito Ramos, 2005; Gutiérrez-Alonso et al., 2015; Martínez Poyatos, 2002; Rodríguez et al., 2003; Valle Aguado et al., 2005). D_{V3} structures suggest left-lateral transpressive deformation and an overall upward extrusion of (Cadomian) basement rocks accommodated along paired shear zones (e.g., pop-ups). The SW Iberian Massif was dominantly affected by this type of shear zones (Azor et al., 1994; Díez Fernández & Pereira, 2016, 2017; Pérez-Cáceres et al., 2016), which in most cases represent the current tectonic boundaries of major paleogeographic zones, such is the case of the Obejo-Valsequillo Domain and Central Iberian Zone in our study area.

4.2. Early Building of the Cadomian Magmatic Arc (D_{C1} and S_{C1})

The oldest evidence of deformation in the study area is twofold. On the one hand, there is foliation trapped within post-kinematic cordierite poikiloblasts (S_{C1}; Figure S2b in Supporting Information S1), which grew in a thermal aureole of Ediacaran meta-granitoids intruded at ∼573 Ma (Ordóñez Casado, 1998). This foliation suggests ductile deformation and metamorphism prior to that age. On the other hand, the Ediacaran igneous bodies were roughly tabular in shape before D_{C2} folding (see Section 3.2.2). The openness and upright geometry inferred for the D_{C2} folds favor the suite of Ediacaran igneous rocks constituting a relatively flat, yet irregular, massif before D_{C2} (Figure 6a).

The variety of rock types that make the Ediacaran igneous suite, along with the primary relationships between them (mingling; Figures S1c and S1d in Supporting Information S1), support a model in which a batholith is constructed by the progressive arrival of many individual plutons to a supra-subduction zone (upper plate). The exotic nature of magmas relative to the sedimentary host (Serie Negra Gp.) is supported by the following: (a) the mafic composition of some igneous rocks, (b) the mingling of such rocks with felsic magmas, (c) the lack of partial melting in the sedimentary host, and (d) the development of thermal metamorphism. We believe that the construction of a batholith the size of the one exposed in the La Serena Massif requires, at least, local extension of the crust to be the host of exotic magmas.

The extension needed to accommodate the arrival of the Ediacaran magma could have left an imprint in the host (e.g., S_{C1}) and plutons (flat-lying tabular shape). Both features can be understood as snapshots of progressive processes. However, extension in this scenario should be regarded as a local process, because the continuous, supra-subduction zone type magmatism that dominates the batholith suggests the arrival of melts to the magmatic axis of the arc (Arenas et al., 2021, 2022; Rojo-Pérez et al., 2024), that is, overall crustal growth. A metamorphic event at ∼573 Ma or older has also been recorded in the nearby Mérida Massif (U-Pb dating in garnet; Arenas et al., 2022), providing further evidence of the coexistence of tectonomagmatic and tectonometamorphic activity during the building of the Cadomian Orogen.

4.3. Advanced Building: Arc Collision (D_{C2} Folding)

The upright geometry of the D_{C2} folds implies horizontal crustal shortening during the second phase of Cadomian deformation. The D_{C2} folds affect the felsic and melanocratic members of the Ediacaran batholith plus the metasedimentary rocks of the Serie Negra Gp., and are unconformably covered by Early Cambrian strata. Accordingly, the age of D_{C2} should be constrained to a range between ∼573 and ∼535 Ma.

During the latest Ediacaran, other sections of the Cadomian Orogen preserved in SW Iberia were subjected to crustal shortening, including ophiolite accretion and obduction in its fore-arc and back-arc sections (Díez Fernández et al., 2019, 2022). The central and northern parts of the Iberian Massif are considered sections of the Cadomian Orogen located inboard Gondwana relative to the rocks in SW Iberia (Díez Fernández et al., 2016; Fuenlabrada et al., 2016, 2021). In these parts of the Iberian Massif, the scarcity of Ediacaran magmatism and the provenance, (turbiditic) nature, and geochemical composition of the sedimentary series are compatible with a paleogeographic location in a wide back-arc section away from the magmatic axis of the Cadomian arc and closer to mainland Gondwana. During the latest Ediacaran period, these sections far from the trench were affected by folding, which led to the uprighting of the sedimentary series (Bandrés, 2001; Capdevila et al., 1971; Díez Balda, 1986; Díez Fernández et al., 2019; Llopis et al., 1970; Martínez Poyatos, 2002; Pieren, 2000). The D_{C2} folds of the study area developed in a section of the arc system probably close to the magmatic axis (see
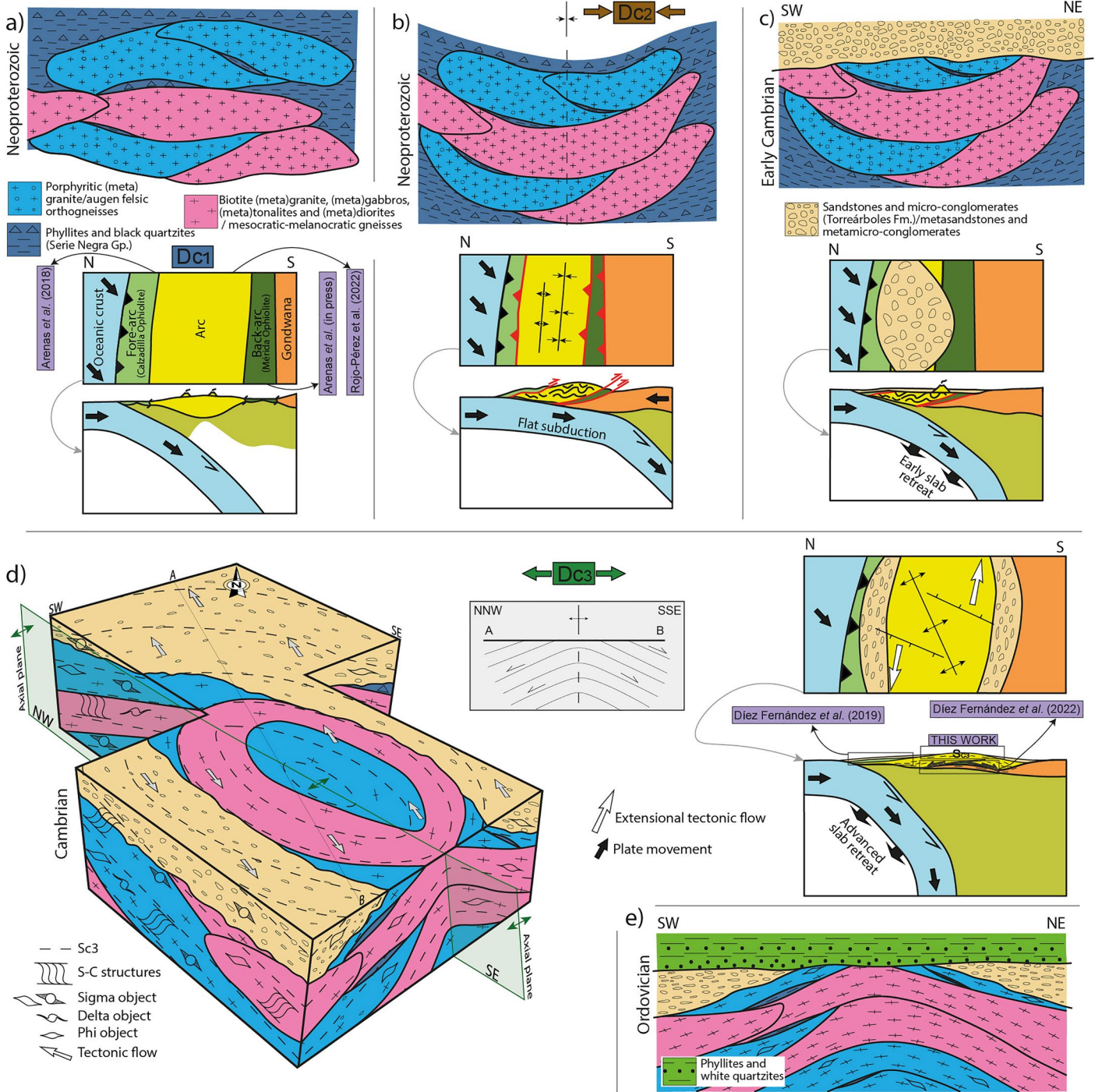
Figure 6. Model showing the tectonic evolution of the Iberian margin of Gondwana during the Ediacaran and Early Paleozoic (in map-view and cross-section) (adapted from Díez Fernández et al. (2022)). (a) A first stage shows the intrusion of Late Ediacaran plutons into the Serie Negra Gp. while the continental arc system grows and broadens (development of fore-arc and back-arc basins). (b) Upright folding affecting the igneous assemblage and its host along the magmatic axis of the arc, while the marginal basins are closed. Overall upper plate compression is framed into a flat subduction event. (c) The resulting mountain belt is eroded away and submerged during the onset of an extensional phase related to the roll-back of the lower plate. The Ediacaran record (sequences and structures) are unconformably covered by Early Cambrian strata (Torreárboles Fm.). (d) To the left, a 3D schematic model and simplified cross-section showing the architecture of the dome generated during the progression of the extensional phase in the upper plate (D$_{C2}$). To the right, a tectonic model that explains the oblique extensional tectonic flow that characterizes the dome in a global context of sinistral plate convergence. (e) Cessation of ductile extensional flow within the dome, erosion, and (unconformable) sedimentation of Ordovician strata during the culmination of the extensional phase that affected this part of the Cadomian Orogen.

discussion in the previous section). Accordingly, by the end of the Ediacaran, the Cadomian Orogen as a whole had experienced horizontal shortening (Figure 6b). Stages of crustal shortening distributed across a significant part of the upper plate to an arc system can be explained by flat subduction events (Stern, 2002). This scenario is considered likely for the latest Ediacaran evolution of the Cadomian Orogen in Iberia, which could have resulted in the collision of the Cadomian arc with mainland Gondwana (Arenas et al., 2018; Bandrés et al., 2004; Henriques et al., 2015; Linnemann et al., 2008; Orejana et al., 2015; Rojo-Pérez et al., 2019), closure of marginal basins (Arenas et al., 2022; Díez Fernández et al., 2019, 2022), and the onset of retro-arc basins (Díez Fernández et al., 2019, 2022; Fuenlabrada et al., 2021; Rojo-Pérez et al., 2024).

The Malcocinado Formation is a volcanic and volcaniclastic series that rests unconformably onto the latest Edia-caran structures, such as those related to ophiolite obduction (Arenas et al., 2022; Díez Fernández et al., 2019; Rojo-Pérez et al., 2024). Such volcanic activity occurred in an active margin, and its age spans the boundary between the latest Ediacaran and the earliest Cambrian (Arenas et al., 2022; Pereira, 2015). Although the Malco-cinado Fm. is missing in the study area, its nature favors a model in which subduction does not cease after an arc collision. The Malcocinado Fm. is unconformably covered by the Early Cambrian series that followed (e.g., Torreárboles Fm.; Liñán, 1984; Rojo-Perez et al., 2024; Figure 6c); therefore, deformation affecting the arc system did not cease either.

4.4. Arc Extensional Collapse (Erosion and D_{C3} Extension)

After D_{C2}, the deposit of Early Cambrian strata (Torreárboles Fm.) unconformably over the remnants of a previ-ously thickened crust indicates that erosion was a significant contributor to the arc dismantlement. Another contributor was the collection of structures formed during D_{C3}, which collectively represent an extensional dome with bi-vergent tectonic flow (La Serena dome). The extensional nature of the flow is typified by the match between the dip-slip inferred from the D_{C3} shear sense and the dip direction of the limb of the D_{C3} dome (Figure 6d). The lack of markedly telescoped isograds in the (cold) metamorphic series suggests that the study area represents the upper structural section of an extensional dome. This section was affected by intense (mylonites) and pervasive D_{C3} strain, but the limited exposure of this Cadomian massif has not allowed us to observe the juxtaposition of low-grade against high-grade crustal sections, as is typical for thermal domes (e.g., Arango et al., 2013; Díez Balda et al., 1995; Escuder Viruete et al., 1994).

We cannot ascertain the onset of the extensional activity that led to the La Serena dome, but it should be later than ∼535 Ma old (youngest age estimation for D_{C2}) and no younger than the Ordovician strata that fossilized the dome (Armorican Quartzite is considered to be Arenig/Floian in age, i.e., ∼477–470 Ma; Gutiérrez-Alonso et al., 2007). The deposit of the Torreárboles Fm. has been framed in the context of Early Cambrian crustal exten-sion (Arenas et al., 2022; Díez Fernández et al., 2015, 2019, 2022; Linnemann et al., 2008; Pereira et al., 2012; Sanchez-Garcia et al., 2003, 2013), which could have occurred during the onset of D_{C3} in the region. Accordingly, the La Serena dome represents the progression of extensional activity that created the Cambrian basins in the first place.

The Cambrian magmatic activity has been divided into two stages. An early extensional stage includes felsic peraluminous rocks derived from crustal melting and minor mantle-derived input, whereas a later extensional stage is characterized by a continuous suite of moderately mafic to acidic rocks with minor intermediate rocks, all of which are derived from various mixtures of crustal- and more abundant mantle-derived magmas (Díez Fernández et al., 2015; Pereira et al., 2023; Rojo-Pérez et al., 2024). The increasing contribution of the mantle suggests that the thickness of the Cadomian orogenic crust progressively attenuated. In our view, the D_{C3} exten-sion represents the structural expression of this process. The eventual involvement of the Torreárboles Fm. into the D_{C3} shear zones indicates upward broadening of the ductile flow during extension. We believe that this illustrates a process of rheological softening throughout the orogen. The upward migration points to an underly-ing thermal anomaly as a likely trigger.

The Cambrian magmas of the early extensional stage are associated with hot lower-crust flow and the formation of high-grade domes in other sections of SW Iberia, which are believed to accommodate passive extension (Díez Fernández et al., 2015; Sánchez-García et al., 2003, 2013). We acknowledge the development of the La Serena dome in the context of hot lower-crust flow. After a period of flat subduction (D_{C2}), the lower plate rolled back and retreated. The progressive nature of this process would have allowed an incremental incursion of a mantle

wedge through the upper/lower plate boundary, thus promoting a thermal anomaly, upper plate extension, and widening of the orogenic system (Díez Fernández et al., 2019, 2022) (Figure 6d). This view is consistent with previous geodynamic models, which suggest oblique incision of an oceanic ridge into the Cadomian Orogen as the trigger for Cambrian extensional tectonics (Linnemann et al., 2008; Sánchez-García et al., 2008). Ridge collision and initial (flat) subduction could explain the overall D_{C2} contraction of the Cadomian upper plate (see Section 4.3), while the subsequent burial of the ridge into the mantle could have created a slab window and the generation of adakitic magma later in the Early Cambrian (Sarrionandia et al., 2020). However, all of these processes require ongoing subduction beneath Gondwana during the Cambrian.

In a model of passive rifting (i.e., extension driven by far-field stresses sourced from plate interactions), a component of lateral movement between tectonic plates induces oblique stretching and extensional tectonic flow oriented obliquely to plate boundaries (roughly defining the orogenic trend) (e.g., Dewey, 2002; Díez Fernández et al., 2012). If lateral plate movement is accompanied by a component of extension normal to plate boundaries (e.g., plates are moving away from each other), the extensional flow will likely tend to be oriented toward the direction in which plates diverge (e.g., Dewey, 2002). In cases where the lateral plate movement includes a component of compression normal to plate boundaries (e.g., derived from ongoing plate convergence and subduction), the extensional flow tends to be reoriented to the strike of the plate boundary (Dewey, 1988; England & Houseman, 1989; Ratschbacher et al., 1989).

D_{C3} extensional flow is characterized by vectors oriented clockwise from both the trend of the La Serena dome (Figure 6d) and the trend of the D_{C2} structures (Figure 4b), which are the two local references constraining the trend of the Cadomian orogenic belt in the study area. Gravitational gradients alone (e.g., pure active rifting) cannot produce such oblique extension in an allegedly linear orogen. The obliqueness of the D_{C3} extensional flow is compatible with a left-lateral component of movement between plates (Figure 6d). We consider the emergence of the La Serena dome to be the contribution of local diapiric flow to the gravity-driven, thermo-mechanical re-equilibration of the Cadomian orogenic crust after D_{C2}. However, the pronounced elongated shape of this (NW-SE-trending) dome indicates NE-SW shortening and/or NW-SE stretching. The NW-SE trend of the dome might have been derived from dominant stretching nearly parallel to the extensional D_{C3} flow, but this would have resulted in constructional strain and linear fabrics (L-tectonites) trending NW-SE (Sullivan, 2013), which are lacking here. The elongated shape of the dome can be derived from NE-SW compression in a setting of ongoing plate convergence (note that the La Serena dome and D_{C2} folds trend similarly). Accordingly, we propose a plate kinematic model for the formation of the dome featured by oblique left-lateral convergence between Gondwana and a downgoing oceanic plate (Figure 6d). The slab retreated from the upper plate, thus creating room for the asthenosphere to penetrate under the base of the Gondwanan continental crust. This would have paved the way for a later stage dominated by active rifting (i.e., a later extensional stage and magmatism with higher mantle influence; Díez Fernández et al., 2015; Sánchez-García et al., 2003, 2008, 2013).

4.5. Integration Within the Cadomian Orogeny of Europe

At the scale of the whole Cadomian record in Europe, a comparison and correlation of major events is possible if we analyze their relative chronology and bearing on the crust, that is, we observe the sequence of events that contributed to crustal growth, thickening, or thinning. Like in Iberia, the record of Cadomian tectonics in the rest of Europe can be divided into contrasting stages.

A first broad stage includes crustal growth in continental arc sections and extension in marginal basins (D_{C1} in this study; from >600 to ~573 Ma). This fits the tectonomagmatic activity recorded in the Bohemian and the Armorican Massifs (Ballèvre et al., 2001; Chantraine et al., 2001; Graviou et al., 1988; Kounov et al., 2012; Linnemann et al., 2014; Sláma et al., 2008; Strachan & Roach, 1990).

A second stage dominated by contraction and basin inversion (D_{C2} in this study; from ~570 to ~540 Ma) is featured by the closure of back-arc basins, the juxtaposition of different terranes and the onset of retro-arc basins in the Iberian Massif. A collection of similar processes has also been proposed to explain the Cadomian record of the Armorican and Bohemian Massifs within that time frame (Ballèvre et al., 2001; Chantraine et al., 2001; Linnemann et al., 2014; Sláma et al., 2008; Strachan & Roach, 1990). Structural data suggest that deformation at this stage formed under a sinistral transpressive setting (Ballèvre et al., 2001; Díez Fernández et al., 2019; Treloar & Strachan, 1990).

A final stage dominated by extension (D_{C3} in this study; from ∼540 to ∼470 Ma) includes the development of a Cambrian unconformity, which is also observed in the Armorican (Cavet et al., 1966) and Bohemian Massifs (Buschmann et al., 2006; Sláma et al., 2008). It is considered to have been formed in a transtensional setting spanning from the latest Ediacaran through to the Cambrian (Ballèvre et al., 2001; Dröst et al., 2004; Linnemann et al., 2000, 2008, 2014; Strachan & Roach, 1990). Out of Iberia, the development of rift basins during this final stage has been linked to Cadomian structural domes (e.g., Linnemann et al., 2014). However, structural evidence about the upwarping and crustal extension inherent to doming is a missing piece in some models (not in ours). On the contrary, the exhumation of migmatites is a process observed in some Cadomian basements (e.g., Ballèvre et al., 2001; Brun & Balé, 1990) and missing in our study area. Therefore, the relationship between Cadomian structural domes and the flow of partially molten crust represents a research line to further our understanding about the Cadomian tectonics in Europe.

The ages of the tectonic and metamorphic events are tentatively older in the Bohemian Massif and in the Armorican Massif compared to those observed in Iberia (Figure 1a). This could be the result of either oblique plate motion during the Cadomian dynamics (Figure 6d), and/or the obliqueness between the boundary of the upper plate (Gondwana) and the ridges, transform faults and plateaus that may have existed in the downgoing slab. In a frame of Cadomian tectonics ruled by left-lateral plate motion, the onset of Cadomian deformation events younger toward southern Europe is compatible with a ridge in the downgoing slab oriented clockwise from the trench (i.e., the external boundary of Gondwana).

5. Conclusions

Restoration of Variscan deformation in the La Serena Massif (SW Iberia, Spain) has revealed three phases of deformation that affected the periphery of Gondwana during the Cadomian Orogeny. The first phase (D_{C1}, prior to 573 Ma) shaped plutons that intruded the continental arc into tabular bodies. The second phase (D_{C2}, 573–535 Ma) is characterized by upright folds and represents additional crustal thickening. The third phase includes the development of an orogen-parallel dome dominated by oblique extensional flow (D_{C3}, ranging between ∼535 and ∼480 Ma). The subduction that controlled the Cadomian orogenesis during the Ediacaran persisted during the Early Paleozoic.

The alternation of contractional and extensional deformation related to the Cadomian cycle in Iberia is aligned with the record of Cadomian deformation in Europe. The stages related to the building, crustal thickening and collapse of the arc system seems rather contemporaneous throughout Europe. This suggests that the plate-scale processes that led to every major event in the Cadomian Orogen must be explained by changes able to operate at the scale of hundreds, even thousands of kilometers along strike (e.g., changes in plate interactions). For instance, alternation between periods dominated by crustal shortening and extension in the upper plate (North African Gondwana) may be due to major changes in the geometry of the subduction plane. Phases dominated by shortening across most of the upper plate (from the fore-arc to the back-arc) are best explained by flat subduction (D_{C2}). A subsequent extension can be framed as a slab retreat stage (D_{C3}). The oblique-to-orogen extensional tectonic flow during this latter stage suggests sinistral convergence. This plate kinematics is also supported by Cadomian sinistral transpressive belts formed in other parts of Europe by the latest Ediacaran, that is, prior to D_{C3}.

Data Availability Statement

Data are available through (Moreno-Martín et al., 2023).

References

Ábalos, B., & Eguíluz, L. (1992). Structural geology of the Mina Afortunada gneiss dome (Badajoz-Córdoba Shear Zone, SW Spain). *Annales Tectonicæ*, *6*, 95–110.

Albert, R., Arenas, R., Gerdes, A., Sánchez Martínez, S., Fernández-Suárez, J., & Fuenlabrada, J. M. (2015). Provenance of the Variscan Upper Allochthon (Cabo Ortegal Complex, NW Iberian Massif). *Gondwana Research*, *28*(4), 1434–1448. https://doi.org/10.1016/j.gr.2014.10.016

Apalategui, O., & Pérez-Lorente, F. (1983). Nuevos datos en el borde meridional de la Zona Centroibérica. El dominio Obejo-Valsequillo-Puebla de la Reina. *Studia Geologica Salmanticensia*, *18*, 193–200.

Apalategui, O., Villalobos, M., & Jorquera de Guindos, A. (1988). *Memoria y mapa geológico de España 1: 50.000* (Vol. 804). Oliva de Mérida.

Arango, C., Díez Fernández, R., & Arenas, R. (2013). Large-scale flat-lying isoclinal folding in extending lithosphere: Santa María de la Alameda dome (Central Iberian Massif, Spain). *Lithosphere*, *5*, 483–500. https://doi.org/10.1130/l270.1

Arenas, R., Díez Fernández, R., Sánchez Martínez, S., Gerdes, A., Fernández-Suárez, J., & Albert, R. (2014). Two-stage collision: Exploring the birth of Pangea in the Variscan terranes. *Gondwana Research*, *25*(2), 756–763. https://doi.org/10.1016/j.gr.2013.08.009

Arenas, R., Fernández-Suárez, J., Montero, P., Díez Fernández, R., Andonaegui, P., Sánchez Martínez, S., et al. (2018). The Calzadilla Ophiolite (SW Iberia) and the Ediacaran fore-arc evolution of the African margin of Gondwana. *Gondwana Research*, *58*, 71–86. https://doi.org/10.1016/j.gr.2018.01.015

Arenas, R., Rojo-Pérez, E., Díez Fernández, R., Albert, R., Novo-Fernández, I., Sánchez Martínez, S., et al. (2022). Opening and closure of Cadomian peri-Gondwanan oceans: Age and evolution of the Mérida Ophiolite (SW Iberia). *International Geology Review*, 1–32. https://doi.org/10.1080/00206814.2022.2129475

Arenas, R., Sánchez Martínez, S., Albert, R., Haissen, F., Fernández-Suárez, J., Pujol-Solà, N., et al. (2021). 100 Myr cycles of oceanic lithosphere generation in peri-Gondwana: Neoproterozoic–Devonian ophiolites from the NW African–Iberian margin of Gondwana and the Variscan Orogen. *Geological Society, London, Special Publications*, *503*(1), 169–184. https://doi.org/10.1144/sp503-2020-3

Arenas, R., Sánchez Martínez, S., Díez Fernández, R., Gerdes, A., Abati, J., Fernández-Suárez, J., et al. (2016). Allochthonous terranes involved in the Variscan suture of NW Iberia: A review of their origin and tectonothermal evolution. *Earth-Science Reviews*, *161*, 140–178. https://doi.org/10.1016/j.earscirev.2016.08.010

Azor, A., Dias Silva, Í., Gómez Barreiro, J., González-Clavijo, E., Martínez Catalán, J. R., Simancas, J. F., et al. (2019). Deformation and structure. In *The geology of Iberia: A geodynamic approach* (pp. 307–348). Springer.

Azor, A., González Lodeiro, F., & Simancas, J. F. (1994). Tectonic evolution of the boundary between the Central Iberian and Ossa-Morena zones (Variscan belt, southwest Spain). *Tectonics*, *13*(1), 45–61. https://doi.org/10.1029/93tc02724

Ballèvre, M., Le Goff, E., & Hébert, R. (2001). The tectonothermal evolution of the Cadomian belt of northern Brittany, France: A Neoproterozoic volcanic arc. *Tectonophysics*, *331*(1), 19–43. https://doi.org/10.1016/S0040-1951(00)00234-1

Bandrés, A. (2001). Evolución geodinámica poliorogénica de los dominios septentrionales de la Zona de Ossa-Morena. Ph.D. (p. 377). University of País Vasco.

Bandrés, A., Eguíluz, L., Gil Ibarguchi, J. I., & Palacios, T. (2002). Geodynamic evolution of a Cadomian arc region: The northern Ossa-Morena zone, Iberian massif. *Tectonophysics*, *352*(1–2), 105–120. https://doi.org/10.1016/s0040-1951(02)00191-9

Bandrés, A., Eguiluz, L., Pin, C., Paquette, J. L., Ordóñez, B., Le Fèvre, B., et al. (2004). The northern Ossa-Morena Cadomian batholith (Iberian Massif): Magmatic arc origin and early evolution. *International Journal of Earth Sciences*, *93*(5), 860–885. https://doi.org/10.1007/s00531-004-0423-6

Bialek, D., Kryza, R., Oberc-Dziedzic, T., & Pin, C. (2014). Cambrian Zawidów granodiorites in the Cadomian Lusatian Massif (Central European Variscides): What do the SHRIMP zircon ages mean? *Journal of Geosciences*, *59*(4), 313–326. https://doi.org/10.3190/jgeosci.179

Blatrix, P., & Burg, J. P. (1981). ^{40}Ar-^{39}Ar dates from Sierra Morena (Southern Spain): Variscan metamorphism and Cadomian orogeny. *Neues Jahrbuch für Mineralogie*, *H.10* (Stuttgart), 470–478.

Brun, J. P., & Balé, P. (1990). Cadomian tectonics in northern Brittany. *Geological Society, London, Special Publications*, *51*(1), 95–114. https://doi.org/10.1144/GSL.SP.1990.051.01.07

Buschmann, B., Elicki, O., & Jonas, P. (2006). The Cadomian unconformity in the Saxo-Thuringian Zone, Germany: Palaeogeographic affinities of Ediacaran (terminal Neoproterozoic) and Cambrian strata. *Precambrian Research*, *147*(3), 387–403. https://doi.org/10.1016/j.precamres.2006.01.023

Capdevila, R., Matte, P., & Paredes, J. (1971). La nature du Précambrien et ses relations avec le Paléozoique dans la Sierra Morena centrale (Sud de l'Espagne). *Comptes Rendus de l'Académie des Sciences de Paris*, *273*, 1359–1362.

Capdevila, R., & Vialette, Y. (1970). Estimation radiométrique de l'âge de la deuxieme phase tectonique hercynienne en Galice Moyenne (Nord-Ouest de l'Espagne). *Comptes Rendus de l'Académie des Sciences*, *270*, 2527–2530.

Castro, A. (1988). Los granitoides deformados de la banda del Guadámez (La Serena, Badajoz). In F. Bea, A. Carnicero, J. C. Gonzalo, M. López-Plaza, & M. D. Rodríguez Alonso (Eds.), *Geología de los granitoides y rocas asociadas del Macizo Hespérico. Libro Homenaje a L.C. García de Figuerola* (pp. 413–426).

Cavet, P., Gruet, M., & Pillet, J. (1966). Sur la présence du Cambrien à Paradoxides à Cléré-sur-Layon (Maine-et-Loire), dans le Nord-Est du Bocage Vendéen (Massif armoricain). *Comptes Rendues Académie des Sciences Paris*, *263*, 1685–1688.

Chantraine, J., Egal, E., Thiéblemont, D., Le Goff, E., Guerrot, C., Ballèvre, M., & Guennoc, P. (2001). The Cadomian active margin (North Armorican Massif, France): A segment of the north Atlantic Panafrican belt. *Tectonophysics*, *331*(1–2), 1–18. https://doi.org/10.1016/s0040-1951(00)00233-x

Dallmeyer, R. D., & Quesada, C. (1992). Cadomian vs. Variscan evolution of the Ossa-Morena Zone (SW Iberia): Field and ^{40}Ar/^{39}Ar mineral age constraints. *Tectonophysics*, *216*(3–4), 339–364. https://doi.org/10.1016/0040-1951(92)90405-u

De Vicente, G., Cunha, P. P., Muñoz-Martín, A., Cloetingh, S. A. P. L., Olaiz, A., & Vegas, R. (2018). The Spanish-Portuguese central system: An example of intense intraplate deformation and strain partitioning. *Tectonics*, *37*(12), 4444–4469. https://doi.org/10.1029/2018tc005204

De Vicente, G., & Vegas, R. (2009). Large-scale distributed deformation controlled topography along the western Africa–Eurasia limit: Tectonic constraints. *Tectonophysics*, *474*(1–2), 124–143. https://doi.org/10.1016/j.tecto.2008.11.026

Dewey, J. F. (1988). Extensional collapse of orogens. *Tectonics*, *7*(6), 1123–1139. https://doi.org/10.1029/TC007i006p01123

Dewey, J. F. (2002). Transtension in arcs and orogens. *International Geology Review*, *44*(5), 402–439. https://doi.org/10.2747/0020-6814.44.5.402

Díaz Azpiroz, M., Castro, A., Fernández, C., López, S., Fernández Caliani, J. C., & Moreno-Ventas, I. (2004). The contact between the Ossa Morena and the South Portuguese zones. Characteristics and significance of the Aracena metamorphic belt, in its central sector between Aroche and Aracena (Huelva). *Journal of Iberian Geology*, *30*, 23–51.

Díez Balda, M. A. (1986). El Complejo Esquisto-Grauváquico, las series paleozoicas y la estructura hercínica al Sur de Salamanca. Ph.D. (p. 162). University of Salamanca.

Díez Balda, M. A., Martínez Catalán, J. R., & Ayarza, P. (1995). Syn-collisional extensional collapse parallel to the orogenic trend in a domain of steep tectonics: The Salamanca detachment zone (Central Iberian Zone, Spain). *Journal of Structural Geology*, *17*(2), 163–182. https://doi.org/10.1016/0191-8141(94)e0042-w

Díez Fernández, R., & Arenas, R. (2015). The Late Devonian Variscan suture of the Iberian Massif: A correlation of high-pressure belts in NW and SW Iberia. *Tectonophysics*, *654*, 96–100. https://doi.org/10.1016/j.tecto.2015.05.001

Díez Fernández, R., Arenas, R., Pereira, M. F., Sánchez-Martínez, S., Albert, R., Martín Parra, L. M., et al. (2016). Tectonic evolution of Variscan Iberia: Gondwana-Laurussia collision revisited. *Earth-Science Reviews*, *162*, 269–292. https://doi.org/10.1016/j.earscirev.2016.08.002

Díez Fernández, R., Arenas, R., Rojo-Pérez, E., Sánchez Martínez, S., & Fuenlabrada, J. M. (2022). Tectonostratigraphy of the Mérida Massif reveals a new Cadomian suture zone exposure in Gondwana (SW Iberia). *International Geology Review*, *64*(3), 405–424. https://doi.org/10.1080/00206814.2020.1858355

Díez Fernández, R., Jiménez-Díaz, A., Arenas, R., Pereira, M. F., & Fernández-Suárez, J. (2019). Ediacaran obduction of a fore-arc ophiolite in SW Iberia: A turning point in the evolving geodynamic setting of peri-Gondwana. *Tectonics*, *38*(1), 95–119. https://doi.org/10.1029/2018tc005224

Díez Fernández, R., & Martínez Catalán, J. R. (2012). Stretching lineations in high-pressure belts: The fingerprint of subduction and subsequent events (Malpica–Tui complex, NW Iberia). *Journal of the Geological Society*, *169*(5), 531–543. https://doi.org/10.1144/0016-76492011-101

Díez Fernández, R., Martínez Catalán, J. R., Gerdes, A., Abati, J., Arenas, R., & Fernández- Suárez, J. (2010). U-Pb ages of detrital zircons from the basal allochthonous units of NW Iberia: Provenance and paleoposition on the northern margin of Gondwana during the Neoproterozoic and Paleozoic. *Gondwana Research*, *18*(2–3), 385–399. https://doi.org/10.1016/j.gr.2009.12.006

Díez Fernández, R., Martínez Catalán, J. R., Gómez Barreiro, J., & Arenas, R. (2012). Extensional flow during gravitational collapse: A tool for setting plate convergence (Padrón migmatitic dome, Variscan belt, NW Iberia). *The Journal of Geology*, *120*(1), 83–103. https://doi.org/10.1086/662735

Díez Fernández, R., Matas, J., Arenas, R., Martín-Parra, L. M., Sánchez Martínez, S., Novo-Fernández, I., & Rojo-Pérez, E. (2021). Two-step obduction of the Porvenir Serpentinite: A cryptic Devonian suture in SW Iberian Massif (Ossa-Morena Complex). In J. Wakabayashi, & Y. Dilek (Eds.), *Plate tectonics, ophiolites, and social significance of geology: A celebration of the career of Eldridge Moores* (Vol. 552, pp. 113–132). GSA Books. https://doi.org/10.1130/2021.2552(07)

Díez Fernández, R., & Pereira, M. F. (2016). Extensional orogenic collapse captured by strike-slip tectonics: Constrains from structural geology and U-Pb geochronology of the Pinhel shear zone (Variscan orogen, Iberian Massif). *Tectonophysics*, *691*, 290–310. https://doi.org/10.1016/j.tecto.2016.10.023

Díez Fernández, R., & Pereira, M. F. (2017). Strike-slip shear zones of the Iberian Massif: Are they coeval? *Geological Society of America Bulletin*, *9*(5), 726–744. https://doi.org/10.1130/l648.1

Díez Fernández, R., Pereira, M. F., & Foster, D. A. (2015). Peralkaline and alkaline magmatism of the Ossa-Morena zone (SW Iberia): Age, source and implications for the Paleozoic evolution of Gondwanan lithosphere. *Lithosphere*, *7*(1), 73–90. https://doi.org/10.1130/l379.1

D'Lemos, R. S., Strachan, R. A., & Topley, C. G. (1990). The Cadomian orogeny in the North Armorican Massif: A brief review. *Geological Society, London, Special Publications*, *51*(1), 3–12. https://doi.org/10.1144/gsl.sp.1990.051.01.01

Dörr, W., Zulauf, G., Fiala, J., Franke, W., & Vejnar, Z. (2002). Neoproterozoic to Early Cambrian history of an active plate margin in the Teplá-Barrandian unit-a correlation of U-Pb isotopic-dilution-TIMS ages (Bohemia, Czech Republic). *Tectonophysics*, *352*(1–2), 65–85. https://doi.org/10.1016/s0040-1951(02)00189-0

Drost, K., Linnemann, U., McNaughton, N., Fatka, O., Kraft, P., Gehmlich, M., et al. (2004). New data on the Neoproterozoic-Cambrian geotectonic setting of the Teplá-Barrandian volcano-sedimentary successions: Geochemistry, U-Pb zircon ages, and provenance (Bohemian Massif, Czech Republic). *International Journal of Earth Sciences*, *93*(5), 742–757. https://doi.org/10.1007/s00531-004-0416-5

Egal, E., Guerrot, C., Le Goff, E., Thiéblemont, D., & Chantraine, J. (1996). *The Cadomian orogeny revisited in northern Brittany (France)* (pp. 281–318). Special Papers-Geological Society of America.

Eguíluz, L. (1988). Petrogénesis de rocas ígneas y metamórficas en el Anticlinorio Burguillos-Monesterio, Macizo Ibérico Meridional. Ph.D. University of País Vasco.

Eguíluz, L., Gil Ibarguchi, J. I., Ábalos, B., & Apraiz, A. (2000). Superposed Hercynian and Cadomian orogenic cycles in the Ossa-Morena zone and related areas of the Iberian Massif. *Geological Society of America Bulletin*, *112*(9), 1398–1413. https://doi.org/10.1130/0016-7606(2000)112<1398:shacoc>2.0.co;2

Eguíluz, L., Ordóñez Casado, B., Gil Ibarguchi, J. I., Apraiz, A., & Ábalos, B. (1999). Superposición de ciclos orogénicos: el ejemplo de la Zona de Ossa-Morena (Macizo Ibérico). *Trabajos de Geología*, *21*, 79–95.

England, P., & Houseman, G. (1989). Extension during continental convergence, with application to the Tibetan Plateau. *Journal of Geophysical Research*, *94*(B12), 17561–17579. https://doi.org/10.1029/jb094ib12p17561

Escuder Viruete, J. E., Arenas, R., & Martínez Catalán, J. R. (1994). Tectonothermal evolution associated with Variscan crustal extension in the Tormes gneiss dome (NW Salamanca, Iberian Massif, Spain). *Tectonophysics*, *238*(1–4), 117–138. https://doi.org/10.1016/0040-1951(94)90052-3

Expósito, I., Simancas, J. F., González Lodeiro, F., Bea, F., Montero, P., & Salman, K. (2003). Metamorphic and deformational imprint of Cambrian-Lower Ordovician rifting in the Ossa-Morena Zone (Iberian Massif, Spain). *Journal of Structural Geology*, *25*(12), 2077–2087. https://doi.org/10.1016/s0191-8141(03)00075-0

Expósito Ramos, I. (2005). Evolución estructural de la mitad septentrional de la Zona de Ossa-Morena y su relación con el límite Zona OssaMorena/Zona Centroibérica. *Terra Nova*, *27*, 1–286.

Fernández-Suárez, J., Gutiérrez-Alonso, G., Jenner, G. A., & Tubrett, M. N. (1999). Crustal sources in Lower Palaeozoic rocks from NW Iberia: Insights from laser ablation U-Pb ages of detrital zircons. *Journal of the Geological Society*, *156*(6), 1065–1068. https://doi.org/10.1144/gsjgs.156.6.1065

Fernández-Suárez, J., Gutiérrez-Alonso, G., Pastor-Galán, D., Hofmann, M., Murphy, J. B., & Linnemamm, U. (2014). The Ediacaran-Early Cambrian detrital zircon record of NW Iberia: Possible sources and paleogeographic constraints. *International Journal of Earth Sciences*, *103*(5), 1335–1357. https://doi.org/10.1007/s00531-013-0923-3

Fossen, H., & Cavalcante, G. C. G. (2017). Shear zones—A review. *Earth-Science Reviews*, *171*, 434–455. https://doi.org/10.1016/j.earscirev.2017.05.002

Franke, W., Cocks, L. R. M., & Torsvik, T. H. (2017). The Palaeozoic Variscan oceans revisited. *Gondwana Research*, *48*, 257–284. https://doi.org/10.1016/j.gr.2017.03.005

Fuenlabrada, J. M., Arenas, R., Díez Fernández, R., González del Tánago, J., Martin-Parra, L. M., Matas, J., et al. (2021). Tectonic setting and isotopic sources (Sm-Nd) of the SW Iberian Autochthon (Variscan Orogen). *Journal of Iberian Geology*, *47*(1), 121–150. https://doi.org/10.1007/s41513-020-00148-7

Fuenlabrada, J. M., Arenas, R., Sánchez Martínez, S., Díaz García, F., & Castiñeiras, P. (2010). A peri-Gondwanan arc in NW Iberia: I: Isotopic and geochemical constraints on the origin of the arc—A sedimentary approach. *Gondwana Research*, *17*(2–3), 338–351. https://doi.org/10.1016/j.gr.2009.09.007

Fuenlabrada, J. M., Pieren, A. P., Díez Fernández, R., Sánchez Martínez, S., & Arenas, R. (2016). Geochemistry of the Ediacaran-Early Cambrian transition in Central Iberia: Tectonic setting and isotopic sources. *Tectonophysics*, *681*, 15–30. https://doi.org/10.1016/j.tecto.2015.11.013

Garrote, A., & Broutin, J. (1979). Le bassin toumaisien de Benajarafe (Province de Cordoue, Espagne). Géologie et premieres données paléobotaniques et palynologiques. *Comptes Rendus du 104 Congres national des Societes savantes (Bordeaux)*, *1*, 175–184.

Graviou, P., Peucat, J. J., Auvray, B., & Vidal, P. (1988). The Cadomian orogeny in the northern Armorican Massif. Petrological and geochronological constraints on a geodynamic model. *Hercynica: Bulletin de la Societe Geologique et Mineralogique de Bretagne*, *4*(1), 1–13.

Gutiérrez-Alonso, G., Collins, A. S., Fernández-Suárez, J., Pastor-Galán, D., González-Clavijo, E., Jourdan, F., et al. (2015). Dating of lithospheric buckling: $^{40}Ar/^{39}Ar$ ages of syn-orocline strike–slip shear zones in northwestern Iberia. *Tectonophysics*, *643*, 44–54. https://doi.org/10.1016/j.tecto.2014.12.009

Gutiérrez-Alonso, G., Fernández-Suárez, J., Gutiérrez-Marco, J. C., Corfu, F., Murphy, J. B., Suárez, M., & Linnemann, U. (2007). U-Pb depositional age for the upper Barrios Formation (Armorican Quartzite facies) in the Cantabrian zone of Iberia: Implications for stratigraphic correlation and paleogeography. *Special Papers—Geological Society of America*, *423*, 287–296.

Hajná, J., Žák, J., & Kachlík, V. (2014). Growth of accretionary wedges and pulsed ophiolitic mélange formation by successive subduction of trench-parallel volcanic elevations. *Terra Nova*, *26*(4), 322–329. https://doi.org/10.1111/ter.12103

Hajná, J., Žák, J., Kachlík, V., & Chadima, M. (2010). Subduction-driven shortening and differential exhumation in a Cadomian accretionary wedge: The Teplá-Barrandian unit, Bohemian Massif. *Precambrian Research*, *176*(1–4), 27–45. https://doi.org/10.1016/j.precamres.2009.10.009

Hajná, J., Žák, J., Kachlík, V., Dörr, W., & Gerdes, A. (2013). Neoproterozoic to early Cambrian Franciscan-type mélanges in the Teplá-Barrandian unit, Bohemian Massif: Evidence of modern-style accretionary processes along the Cadomian active margin of Gondwana? *Precambrian Research*, *224*, 653–670. https://doi.org/10.1016/j.precamres.2012.11.007

Henriques, S. B. A., Neiva, A. M. R., Ribeiro, M. L., Dunning, G. R., & Tajčmanová, L. (2015). Evolution of a Neoproterozoic suture in the Iberian Massif, Central Portugal: New U-Pb ages of igneous and metamorphic events at the contact between the Ossa Morena Zone and Central Iberian Zone. *Lithos*, *220*, 43–59. https://doi.org/10.1016/j.lithos.2015.02.001

Herranz Araújo, A. (1985). El precámbrico y su cobertera paleozoica en la región centro-oriental de la provincia de Badajoz. Ph.D (p. 497). University Complutense of Madrid, Seminarios de Estratigrafía, Tomo II.

Insúa Márquez, M., Carvajal Menéndez, A., Apalategui Isasa, O., Huerta Carmona, J., & Matía Villarino, G. (1991). *Memoria y mapa geológico de España 1: 50.000* (p. 805). Castuera.

Jolivet, L., Augier, R., Faccenna, C., Negro, F., Rimmele, G., Agard, P., et al. (2008). Subduction convergence and the mode of backarc extension in the Mediterranean region. *Bulletin de la Societe Geologique de France*, *179*(6), 525–550. https://doi.org/10.2113/gssgfbull.179.6.525

Kounov, A., Graf, J., von Quadt, A., Bernoulli, D., Burg, J.-P., Seward, D., et al. (2012). Evidence for a "Cadomian" ophiolite and magmatic-arc complex in SW Bulgaria. *Precambrian Research*, *212–213*, 275–295. https://doi.org/10.1016/j.precamres.2012.06.003

Liñán, E. (1984). Los icnofósiles de la Formación Torreárboles (¿Precámbrico? Cámbrico Inferior) en los alrededores de Fuente de Cantos, Badajoz. *Cuadernos do Laboratorio Xeoloxico de Laxe*, *8*, 47–74.

Liñán, E., & Palacios, T. (1983). Aportaciones micropaleontológicas para el conocimiento del límite Precámbrico-Cámbrico en la Sierra de Córdoba, España. *Comunicações dos Serviços Geológicos de Portugal*, *69*, 227–234.

Liñán, E., Palacios, T., & Perejón, A. (1984). Precambrian—Cambrian boundary and correlation from southwestern and central part of Spain. *Geological Magazine*, *121*(03), 221–228. https://doi.org/10.1017/S0016756800028284

Lindner, M., & Finger, F. (2018). Geochemical characteristics of the Late Proterozoic Spitz granodiorite gneiss in the Drosendorf Unit (Southern Bohemian Massif, Austria) and implications for regional tectonic interpretations. *Journal of Geosciences*, *63*(4), 345–362. https://doi.org/10.3190/jgeosci.271

Linnemann, U., Gehmlich, M., Tichomirowa, M., Buschmann, B., Nasdala, L., Jonas, P., et al. (2000). From Cadomian subduction to Early Palaeozoic rifting: The evolution of Saxo-Thuringia at the margin of Gondwana in the light of single zircon geochronology and basin development (Central European Variscides, Germany). *Geological Society, London, Special Publications*, *179*(1), 131–153. https://doi.org/10.1144/gsl.sp.2000.179.01.10

Linnemann, U., Gerdes, A., Hofmann, M., & Marko, L. (2014). The Cadomian Orogen: Neoproterozoic to Early Cambrian crustal growth and orogenic zoning along the periphery of the West African Craton—Constraints from U–Pb zircon ages and Hf isotopes (Schwarzburg Antiform, Germany). *Precambrian Research*, *244*, 236–278. https://doi.org/10.1016/j.precamres.2013.08.007

Linnemann, U., Pereira, F., Jeffries, T. E., Drost, K., & Gerdes, A. (2008). The Cadomian Orogeny and the opening of the Rheic Ocean: The diacrony of geotectonic processes constrained by LA-ICP-MS U-Pb zircon dating (Ossa-Morena and Saxo-Thuringian Zones, Iberian and Bohemian Massifs). *Tectonophysics*, *461*(1–4), 21–43. https://doi.org/10.1016/j.tecto.2008.05.002

Llopis, N., San José, M. A., & Herranz, P. (1970). Notas sobre una discordancia posiblemente precámbrica al SE de la provincia de Badajoz y sobre la edad de las series paleozoicas circundantes. *Boletin Geologico y Minero*, *81*, 586–592.

Martínez Catalán, J. R., Arenas, R., Abati, J., Sánchez Martínez, S., Díaz García, F., Fernández Suárez, J., et al. (2009). A rootless suture and the loss of the roots of a mountain chain: The Variscan belt of NW Iberia. *Comptes Rendus Geoscience*, *341*(2–3), 114–126. https://doi.org/10.1016/j.crte.2008.11.004

Martínez Catalán, J. R., Rubio Pascual, F. J., Díez Montes, A., Díez Fernández, R., Gómez Barreiro, J., Dias da Silva, Í., et al. (2014). The late Variscan HT/LP metamorphic event in NW and Central Iberia: Relationships to crustal thickening, extension, orocline development and crustal evolution. In K. Schulmann, J. R. Martínez Catalán, J. M. Lardeaux, V. Janoušek, & G. Oggiano (Eds.), *The Variscan orogeny: Extent, timescale and the formation of the European crust* (pp. 225–247). Geological Society of London Special Publication.

Martínez Catalán, J. R., Schulmann, K., & Ghienne, J. F. (2021). The Mid-Variscan Allochthon: Keys from correlation, partial retrodeformation and plate-tectonic reconstruction to unlock the geometry of a non-cylindrical belt. *Earth-Science Reviews*, *220*, 1–65. https://doi.org/10.1016/j.earscirev.2021.103700

Martínez Poyatos, D. (2002). Estructura del borde meridional de la Zona Centroibérica y su relación con el contacto entre las Zonas Centroibérica y de Ossa-Morena. Ph.D. Thesis. University of Granada.

Martín Parra, L. M., González Lodeiro, F., Martínez Poyatos, D., & Matas, J. (2006). The Puente Génave-Castelo de Vide shear zone (southern Central Iberian Zone, Iberian Massif): Geometry, kinematics and regional implications. *Bulletin de la Societe Geologique de France*, *177*(4), 191–202. https://doi.org/10.2113/gssgfbull.177.4.191

Matte, P. (1991). Accretionary history and crustal evolution of the Variscan belt in Western Europe. *Tectonophysics*, *196*(3–4), 309–337. https://doi.org/10.1016/0040-1951(91)90328-p

Matte, P. (2001). The Variscan collage and orogeny (480-290 Ma) and the tectonic definition of the Armorica microplate: A review. *Terra Nova*, *13*(2), 122–128. https://doi.org/10.1046/j.1365-3121.2001.00327.x

Moreno-Martín, D., Díez Fernández, R., Arenas, R., Rojo-Pérez, E., Novo-Fernández, I., & Sánchez Martínez, S. (2023). "Structural data from La Serena Massif" (version 1) [Dataset]. Mendeley Data. https://doi.org/10.17632/ntmzh3p5ny.1

Moreno-Martín, D., Díez Fernández, R., de Vicente, G., Fernández Rodríguez, C., & Gómez Barreiro, J. (2022). Orogenic reworking and reactivation in Central Iberia: A record of Variscan, Permian and Alpine tectonics. *Tectonophysics*, *843*, 229601. https://doi.org/10.1016/j.tecto.2022.229601

Murphy, J. B., Gutierrez-Alonso, G., Nance, R. D., Fernandez-Suarez, J., Keppie, J. D., Quesada, C., et al. (2006). Origin of the Rheic Ocean: Rifting along a Neoproterozoic suture? *Geology*, *34*(5), 325–328. https://doi.org/10.1130/g22068.1

Nance, R. D., Gutiérrez-Alonso, G., Keppie, J. D., Linnemann, U., Murphy, J. B., Quesada, C., et al. (2010). Evolution of the Rheic Ocean. *Gondwana Research*, *17*(2–3), 194–222. https://doi.org/10.1016/j.gr.2009.08.001

Nance, R. D., Murphy, J. B., Strachan, R. A., D'Lemos, R. S., & Taylor, G. K. (1991). Late Proterozoic tectonostratigraphic evolution of the Avalonian and Cadomian terranes. *Precambrian Research*, *53*(1–2), 41–78. https://doi.org/10.1016/0301-9268(91)90005-u

Ordóñez Casado, B. (1998). Geochronological studies of the Pre-Mesozoic basement of the Iberian Massif: The Ossa Morena zone and the Allochthonous Complexes within the Central Iberian zone. Ph.D. (p. 233). University of ETH Zurich.

Orejana, D., Merino Martínez, E., Villaseca, C., & Andersen, T. (2015). Ediacaran-Cambrian paleogeography and geodynamic setting of the Central Iberian Zone: Constraints from coupled U-Pb-Hf isotopes of detrital zircons. *Precambrian Research*, *261*, 234–251. https://doi.org/10.1016/j.precamres.2015.02.009

Pereira, M. F. (2015). Potential sources of Ediacaran strata of Iberia: A review. *Geodinamica Acta*, *27*, 1–14. https://doi.org/10.1080/09853111.2014.957505

Pereira, M. F., Chichorro, M., Linnemann, U., Eguiluz, L., & Silva, J. B. (2006). Inherited arc signature in Ediacaran and Early Cambrian basins of the Ossa-Morena zone (Iberian Massif, Portugal): Paleogeographic link with European and North African Cadomian correlatives. *Precambrian Research*, *144*(3–4), 297–315. https://doi.org/10.1016/j.precamres.2005.11.011

Pereira, M. F., Chichorro, M., Williams, I. S., Silva, J. B., Fernandez, C., Díaz Azpiroz, M., et al. (2009). Variscan intra-orogenic extensional tectonics in the Ossa-Morena Zone (Evora-Aracena-Lora del Rio metamorphic belt, SW Iberian Massif): SHRIMP zircon U-Th-Pb geochronology. *Geological Society, London, Special Publications*, *327*(1), 215–237. https://doi.org/10.1144/sp327.11

Pereira, M. F., Gama, C., Dias da Silva, Í., Fuenlabrada, J. M., & El Houicha, M. (2023). Cadomian arc recycling along the northern Gondwana margin: Source-inherited composition of Miaolingian rift-related rhyolitic rocks (Ossa-Morena Zone, SW Iberia). *Journal of African Earth Sciences*, *201*, 104887. https://doi.org/10.1016/j.jafrearsci.2023.104887

Pereira, M. F., Solá, A. R., Chichorro, M., Lopes, L., Gerdes, A., & Silva, J. B. (2012). North-Gondwana assembly, break-up and paleogeography: U–Pb isotope evidence from detrital and igneous zircons of Ediacaran and Cambrian rocks of SW Iberia. *Gondwana Research*, *22*(3–4), 866–881. https://doi.org/10.1016/j.gr.2012.02.010

Pérez-Cáceres, I., Simancas, J. F., Martínez Poyatos, D., Azor, A., & González Lodeiro, F. (2016). Oblique collision and deformation partitioning in the SW Iberian Variscides. *Solid Earth*, *7*(3), 857–872. https://doi.org/10.5194/se-7-857-2016

Pieren, A. P. (2000). Las sucesiones anteordovícicas de la región oriental de la provincia de Badajoz y área contigua de la de Ciudad Real. Ph.D. (p. 620). Complutense University of Madrid.

Quesada, C. (1990). Precambrian successions in SW Iberia: Their relationship to 'Cadomian' orogenic events. In D. R. Lemos, R. A. Strachan, & C. G. Topley (Eds.), *The Cadomian Orogeny* (Vol. 51, pp. 353–362). Geological Society, Special Publication.

Quesada, C. (2006). The Ossa-Morena Zone of the Iberian Massif: A tectonostratigraphic approach to its evolution. *Zeitschrift der Deutschen Gesellschaft für Geowissenschaften*, *157*(4), 585–595. https://doi.org/10.1127/1860-1804/2006/0157-0585

Ramsay, J. G. (1967). *Folding and fracturing of rocks*. McGraw-Hill.

Ratschbacher, L., Frisch, W., Neubauer, F., Schmid, S. M., & Neugebauer, J. (1989). Extension in compressional orogenic belts: The eastern Alps. *Geology*, *17*(5), 404–407. https://doi.org/10.1130/0091-7613(1989)017<0404:eicobt>2.3.co;2

Ribeiro, A., Munhá, J., Dias, R., Mateus, A., Pereira, E., Ribeiro, L., et al. (2007). Geodynamic evolution of the SW Europe Variscides. *Tectonics*, *26*(6), 1–24. https://doi.org/10.1029/2006tc002058

Rodríguez, J., Cosca, M. A., Gil Ibarguchi, J. I., & Dallmeyer, R. D. (2003). Strain partitioning and preservation of ^{40}Ar/^{39}Ar ages during Variscan exhumation of a subducted crust (Malpica-Tui complex, NW Spain). *Lithos*, *70*(3–4), 111–139. https://doi.org/10.1016/s0024-4937(03)00095-1

Rodríguez-Alonso, M. D., Peinado, M., López-Plaza, M., Franco, P., Carnicero, A., & Gonzálo, J. C. (2004). Neoproterozoic-Cambrian synsedimentary magmatism in the Central Iberian Zone (Spain): Geology, petrology and geodynamic significance. *International Journal of Earth Sciences*, *93*(5), 897–920. https://doi.org/10.1007/s00531-004-0425-4

Rojo-Pérez, E., Arenas, R., Fuenlabrada, J. M., Novo-Fernández, I., Sánchez Martínez, S., Moreno-Martín, D., & Díez Fernández, R. (2024). Lower Cambrian magmatism in the SW Iberian sector of the African–Gondwana margin: Geochemical and isotopic keys to incipient tectonic switching. *Geological Society, London, Special Publications*, *542*(1), SP542–2022. https://doi.org/10.1144/SP542-2022-294

Rojo-Pérez, E., Arenas, R., Fuenlabrada, J. M., Sánchez Martínez, S., Martín Parra, L. M., Matas, J., et al. (2019). Contrasting isotopic sources (Sm-Nd) of Late Ediacaran series in the Iberian Massif: Implications for the Central Iberian-Ossa Morena boundary. *Precambrian Research*, *324*, 194–207. https://doi.org/10.1016/j.precamres.2019.01.021

Rojo-Pérez, E., Fuenlabrada, J. M., Linnemann, U., Arenas, R., Sánchez Martínez, S., Díez Fernández, R., et al. (2021). Geochemistry and Sm–Nd isotopic sources of Late Ediacaran siliciclastic series in the Ossa–Morena Complex: Iberian–Bohemian correlations. *International Journal of Earth Sciences*, *110*(2), 467–485. https://doi.org/10.1007/s00531-020-01963-0

Rojo-Pérez, E., Linnemann, U., Hofmann, M., Fuenlabrada, J. M., Zieger, J., Fernández-Suárez, J., et al. (2022). U-Pb geochronology and isotopic geochemistry of adakites and related magmas in the Ediacaran arc section of the SW Iberian Massif: The role of subduction erosion cycles in peri-Gondwanan arcs. *Gondwana Research*, *109*, 89–112. https://doi.org/10.1016/j.gr.2022.04.011

Rubio-Ordóñez, A., Gutiérrez-Alonso, G., Valverde-Vaquero, P., Cuesta, A., Gallastegui, G., Gerdes, A., & Cárdenes, V. (2015). Arc-related Ediacaran magmatism along the northern margin of Gondwana: Geochronology and isotopic geochemistry from northern Iberia. *Gondwana Research*, *27*(1), 216–227. https://doi.org/10.1016/j.gr.2013.09.016

Rubio Pascual, F. J., Arenas, R., Martínez Catalán, J. R., Fernández, L. R. R., & Wijbrans, J. R. (2013). Thickening and exhumation of the Variscan roots in the Iberian Central System: Tectonothermal processes and ^{40}Ar/^{39}Ar ages. *Tectonophysics*, *587*, 207–221. https://doi.org/10.1016/j.tecto.2012.10.005

Rubio Pascual, F. J., López-Carmona, A., & Arenas, R. (2016). Thickening vs. extension in the Variscan belt: P-T modelling in the Central Iberian autochthon. *Tectonophysics*, *681*, 144–158. https://doi.org/10.1016/j.tecto.2016.02.033

Sánchez-Cela, V., & Gabaldón, V. (1977). *Memoria y mapa geológico de España 1: 50.000* (p. 831). Zalamea de la Serena.

Sánchez-García, T., Bellido, F., & Quesada, C. (2003). Geodynamic setting and geochemical signatures of Cambrian-Ordovician rift-related igneous rocks (Ossa-Morena Zone, SW Iberia). *Tectonophysics*, *365*(1–4), 233–255. https://doi.org/10.1016/s0040-1951(03)00024-6

Sánchez-García, T., Pereira, M. F., Bellido, F., Chichorro, M., Silva, J. B., Valverde-Vaquero, P., et al. (2013). Early Cambrian granitoids of North Gondwana margin in the transition from a convergent setting to intra-continental rifting (Ossa-Morena Zone, SW Iberia). *International Journal of Earth Sciences*, *103*(5), 1203–1218. https://doi.org/10.1007/s00531-013-0939-8

Sánchez-García, T., Quesada, C., Bellido, F., Dunning, G. R., & González del Tánago, J. (2008). Two-step magma flooding of the upper crust during rifting: The Early Paleozoic of the Ossa Morena Zone (SW Iberia). *Tectonophysics*, *461*(1–4), 72–90. https://doi.org/10.1016/j.tecto.2008.03.006

Sánchez-Lorda, M. E., Ábalos, B., García de Madinabeitia, S., Eguíluz, L., Gil Ibarguchi, J. I., & Paquette, J. L. (2016). Radiometric discrimination of pre-Variscan amphibolites in the Ediacaran Serie Negra (Ossa-Morena Zone, SW Iberia). *Tectonophysics*, *681*, 31–45. https://doi.org/10.1016/j.tecto.2015.09.020

Sarrionandia, F., Ábalos, B., Errandonea-Martin, J., Eguíluz, L., Santos-Zalduegui, J. F., García de Madinabeitia, S., et al. (2020). Ediacaran-Earliest Cambrian arc-tholeiite and adakite associations of the Malcocinado Formation (Ossa-Morena Zone, SW Spain): Juvenile continental crust and deep crustal reworking in northern Gondwana. *Lithos*, *372*, 105683. https://doi.org/10.1016/j.lithos.2020.105683

Simancas, J. F., Azor, A., Martínez-Poyatos, D., Tahiri, A., El Hadi, H., González-Lodeiro, F., et al. (2009). Tectonic relationships of Southwest Iberia with the allochthons of Northwest Iberia and the Moroccan Variscides. *Comptes Rendus Geoscience*, *341*(2–3), 103–113. https://doi.org/10.1016/j.crte.2008.11.003

Sláma, J., Dunkley, D. J., Kachlík, V., & Kusiak, M. A. (2008). Transition from island-arc to passive setting on the continental margin of Gondwana: U-Pb zircon dating of Neoproterozoic metaconglomerates from the SE margin of the Teplá-Barrandian Unit, Bohemian Massif. *Tectonophysics*, *461*(1–4), 44–59. https://doi.org/10.1016/j.tecto.2008.03.005

Stampfli, G. M., Hochard, C., Vérard, C., Wilhem, C., & von Raumer, J. (2013). The formation of Pangea. *Tectonophysics*, *593*, 1–19. https://doi.org/10.1016/j.tecto.2013.02.037

Stern, R. J. (2002). Subduction zones. *Reviews of Geophysics*, *40*(4), 1012. https://doi.org/10.1029/2001rg000108

Strachan, R. A., & Roach, R. A. (1990). Tectonic evolution of the Cadomian belt in north Brittany. *Geological Society, London, Special Publications*, *51*(1), 133–150. https://doi.org/10.1144/GSL.SP.1990.051.01.09

Sullivan, W. A. (2013). L tectonites. *Journal of Structural Geology*, *50*, 161–175. https://doi.org/10.1016/j.jsg.2012.01.022

Treloar, P. J., & Strachan, R. A. (1990). Cadomian strike-slip tectonics in NE Brittany. *Geological Society, London, Special Publications*, *51*(1), 151–168. https://doi.org/10.1144/GSL.SP.1990.051.01.10

Valle Aguado, B., Azevedo, M. R., Schaltegger, U., Martínez Catalán, J. R., & Nolan, J. (2005). U-Pb zircon and monazite geochronology of Variscan magmatism related to syn-convergence extension in Central Northern Portugal. *Lithos*, *82*(1–2), 169–184. https://doi.org/10.1016/j.lithos.2004.12.012

Von Raumer, J. F., & Stampfli, G. M. (2008). The birth of the Rheic Ocean—Early Palaeozoic subsidence patterns and subsequent tectonic plate scenarios. *Tectonophysics*, *461*(1–4), 9–20. https://doi.org/10.1016/j.tecto.2008.04.012

References From the Supporting Information

Blenkinsop, T. G., & Treloar, P. J. (1995). Geometry, classification and kinematics of S-C and S-C′ fabrics in the Mushandike area, Zimbabwe. *Journal of Structural Geology*, *17*(3), 397–408. https://doi.org/10.1016/0191-8141(94)00063-6

Cardozo, N., & Allmendinger, R. W. (2013). Spherical projections with OSXStereonet. (Version 11.3.6) [Software]. *Computers & Geosciences*, *51*, 193–205. https://doi.org/10.1016/j.cageo.2012.07.021

Gómez Barreiro, J., Martínez Catalán, J. R., Díez Fernández, R., Arenas, R., & Díaz García, F. (2010). Upper crust reworking during gravitational collapse: The Bembibre-Pico Sacro detachment system (NW Iberia). *Journal of the Geological Society*, *167*, 769–784. https://doi.org/10.1144/0016-76492009-160

Lister, G. S., & Snoke, A. W. (1984). S-C mylonites. *Journal of Structural Geology*, *6*, 617–638.

Means, W. D., Hobbs, B. E., Lister, G. S., & Williams, P. F. (1980). Vorticity and non-coaxiality in progressive deformations. *Journal of Structural Geology*, *2*, 371–378.